UNIVERSITY OF
EASTERN FINLAND

Emissions of CO_2 and CH_4 and source identification along warming gradients in the spruce forest of Iceland

Katri Ylä-Soininmäki
Environmental Science
University of Eastern Finland
Faculty of Science and Forestry
Department of Environmental
and Biological Sciences
6.3.2023

The University of Eastern Finland, Faculty of Science and Forestry
Department of Environmental and Biological Sciences
Biology of Environmental Change
Ylä-Soininmäki, Katri: Emissions of CO_2 and CH_4 and source identification along warming gradients in the spruce forest of Iceland
Thesis, 62 pages, 1 appendix (3 pages)
Thesis instructors: Research Director Christina Biasi (PhD), Professor Marja Maljanen, Researcher Carolina Voigt (PhD), and Junior Researcher Johanna Kerttula
March 2023

Keywords: $\delta^{13}C$, emissions, biological respiration, warming, volcanic soil

ABSTRACT

Biological respiration is the main process of releasing C sequestered in soils into the atmosphere. Natural temperature gradients have been widely used to study the effects of warming on GHG fluxes from soils. These temperature gradients can be found in geothermal areas such as Iceland. However, geothermal areas release abiotic CO_2 and CH_4, which must be considered when interpreting the temperature sensitivity of soil respiration. As implemented in this thesis, isotope techniques are the only method for separating the abiotic and biotic fluxes.

In this thesis, CO_2 and CH_4 fluxes and their $\delta^{13}C$ values were measured with the static enclosed chamber method at the ForHot research communities study site, which is divided into 6 temperature transects from ambient temperatures up to +40°C of warming. This thesis aimed to investigate the temperature sensitivity of biological respiration and CH_4 responses to medium-term warming (14 years) in the geothermal spruce forest of Iceland, along the natural temperature gradient. To achieve this, first trenching method was applied to execute the roots and thus study the biological respiration solely. Secondly, abiotic, and biotic CO_2 fluxes were separated with a two-pool isotope mixing model.

Results showed that strong geological CO_2 fluxes were released from the warmest transects and thus highlighted the importance of source partitioning when studying the temperature effects on microbial respiration in geothermal temperature gradients. No two-pool isotope mixing model was applied for CH_4 since CH_4 oxidation is against the mixing model assumptions of spatially and temporarily invariable end-member values. However, there was a strong indication of abiotic CH_4 released from the warmest transects (+30°C), based on the δ-values measured for CH_4 and geothermal vents. There was only CH_4 uptake observed within the moderate temperature increase and emissions from the warmest transects with values ranging from -1.94 mg CH_4 m^{-2} day^{-1} (net uptake) to 2.43 mg CH_4 mg m^{-2} day^{-1} (emissions). There were no significant differences in the CH_4 uptake rates mainly due to the low-temperature sensitivity of CH_4 uptake.

It was assumed that the trenching method worked, and that root respiration was negligible since CO_2 fluxes measured from the trenched plots were lower in all the transects compared to the non-trenched plots. Unlike expected, no significant differences in the biological fluxes were found within the moderate temperature increase. The biological fluxes stayed within an average of 460 mg CO_2 m^{-2} h^{-1} with moderate temperature increase and significantly decreased with a temperature increase of +5°C and +30°C. The highest fluxes (520.62 mg CO_2 $m^{-2}h^{-1}$) were measured with +1.5°C of warming the and lowest (47.83 mg CO_2 $m^{-2}h^{-1}$) with +5°C. There are several factors affecting biological respiration. Here, the amount of available carbon seemed to be the most significant limiting factor. More studies are required considering both CO_2 and CH_4 to be able to predict the ecological and biogeochemical responses to global warming. However, the results of this thesis provide valuable insight into the adaptation of microbial respiration to the warming climate.

Foreword

This thesis was part of the KYT-2022 NAT-LAB 14C project. The sampling and measurements were conducted at the ForHot study site managed by the Agricultural University of Iceland in July 2022. The analyses were done in the autumn of 2022 at the University of Eastern Finland at Kuopio.

First, I would like to thank all of my supervisors: Christina Biasi, Carolina Voigt, Marja Maljanen, and Johanna Kerttula for all the guidance and help. Additionally, I would like to thank Maija Marushchak for the persistent help with the data processing and the ForHot community for all the assistance while we were sampling in Iceland.

Lastly, I want to thank my closest people, without your support, this thesis would have not been finished. The greatest thanks go home, to Olli, who has been tirelessly sympathetic and encouraged me during this project.

Reykjavik 6.3.2023
Katri Ylä-Soininmäki

Abbreviations

C	Carbon
FN	Sitka spruce plantation site
GHG	Greenhouse gas
GN	Grassland site (new)
GO	Grassland site (old)
IAEA	International Atomic Energy Agency
IPCC	The Intergovernmental Panel on Climate Change
IRGA	Infra-red gas analyzer
NEE	Net ecosystem exchange
OTC	Open top chamber
PPB	Parts per billion
PPM	Parts per million
SOC	Soil organic carbon
SOM	Soil organic matter
TC	Total carbon
TN	Total nitrogen
TOC	Total organic carbon

Contents

1 Introduction

Soils in the northern latitudes are significant carbon stocks and are most affected by global warming (Rantanen et al. 2022). There is a high probability that the microbial activity, and furthermore the release of soil C (CO_2), will increase due to climate warming (Marañón-Jiménez et al. 2018). The effects of warming on CH_4 emissions are less well known, but crucial, since CH_4 is 30 times stronger GHG than CO_2 (IPCC 2021). Natural temperature gradients can be used to study the effects of soil warming. These gradients are rare within a geographical region but can be found e.g., in Iceland, where volcanic activity enhances soil temperatures (O'Gorman et al. 2014). However, it has been shown that geothermal areas release abiotic CO_2 and that these non-biotic fluxes can form a significant part of the total CO_2 emitted (Maljanene et al. 2020). Carbon dioxide efflux and its $\delta^{13}C$ value differ a lot between biotic and abiotic CO_2. To avoid false interpretations of temperature dependencies of respiratory fluxes when implementing these natural temperature gradients, there is a need to separate abiotic and biotic GHG fluxes. This can be achieved by stable isotope analysis as done in this thesis.

The ForHot study site, managed by the Agricultural University of Iceland, is a unique natural laboratory offering varied opportunities for climate research (https://forhot.is/). Maljanen et al. implemented the stable isotope method and researched the role of the abiotic source of CO_2 fluxes in southern Iceland at the ForHot study site. However, the mechanisms and especially the portion of vegetation-derived CO_2 in overall CO_2 emissions in warming areas were not determined. To specify the effects of soil warming on the sensitivity of biological respiration, trenching experiments were initiated in the Iceland study site in 2021, allowing a detailed investigation of temperature effects on microbial respiration rates solely. In this thesis, I aim to investigate the effects of natural soil warming on soil microbial respiration rates. The purpose of this thesis is to gain valuable information on the responses of soil decomposition processes to medium-term natural warming and provide more insights into mechanisms underlying the responses of CO_2 and CH_4 fluxes. I aim to identify the sources of CO_2 fluxes by firstly eliminating the effects of vegetation by removing the roots from the soil samples, secondly partitioning the CO_2 fluxes with isotope approaches, and finally accurately determining the temperature sensitivity of biological respiration.

2 Literature Review

2.1 Climate change and northern ecosystems

There is scientific consensus that human actions have warmed the biosphere. Global greenhouse gas (GHG) emissions have been significantly increasing since pre-industrial times. Carbon dioxide (CO_2), methane (CH_4), and nitrous oxide (N_2O) are the main anthropogenic GHGs. At the end of the year 2019, these gases had reached annual averages of 410 ppm (CO_2), 1866 ppb (CH_4), and 332 ppb (N_2O) (IPCC 2021). Each of the last four decades has been consecutively warmer than the decade preceding it (IPCC 2021). Ecological effects of warming have already been observed at the ecosystem scale, e.g., increased drought, ocean acidification, thawing of permafrost and associated loss of soil carbon, as well as changes and loss of species, e.g., altered timing of life cycle events, loss of species and spatial range shifts. (O'Gorman et al. 2014; IPCC 2021).

It is estimated that climate change will be more rapid and the effects stronger in the northern hemisphere (Rantanen et. al 2022). In both hemispheres, climate zones have shifted poleward. On average, the growing season has been prolonged by two days per decade since the 1950s in the Northern Hemisphere (IPCC 2021). Compared to the global average, over the past decades, warming has been nearly twice as large in the North, and four times as large in the Arctic region (Rantanen et al. 2022). It is estimated that the average temperature can increase by up to + 5°C by the year 2100 (IPCC 2021). To be able to predict the ecological and biogeochemical responses to warming accurately, we will need to gain more understanding of the evolutionary, physiological, and ecological responses to warming, both on spatial and temporal scales. (O'Gorman et al. 2014).

2.2 Carbon cycle

Carbon is the basic building block for life. Apart from the carbon that is stored in rocks, significant amounts of carbon are stored in the oceans, plants, and organisms, as well as in soils.

Particularly northern soils store a considerable amount of the Earth's soil carbon reservoir, approximately 1307 Pg C (about 30 %) (Hugelius et al. 2014). Carbon moving between these reservoirs forms the carbon cycle. The carbon cycle consists of slow and fast processes, that are explained in more detail in the following chapters.

Humans have a significant impact on the carbon cycle (Riebeek 2011). Moreover, carbon is a key element in the global climate crisis, since it is the base of the most abundant and significant GHG, carbon dioxide (CO_2) (IPCC 2021). The main sources of CO_2 are the emissions from human activities, most significantly the combustion of fossil fuels. After CO_2, methane (CH_4) is the second most important GHG. Though the abundance of CH_4 is much lower in the atmosphere compared to CO_2, CH_4 is approximately 30 times stronger than CO_2 on a 100-year timescale (IPCC 2021). It is estimated that natural sources of CH_4 account for approximately 40 % of global CH_4 emissions. The most important ones of these are wetlands, termites, and several geological sources (Reay et al. 2010).

2.2.1 Fast carbon cycle

The fast carbon cycle sometimes also called the biological carbon cycle, occurs in the Earth's living matter through different life forms, and moves carbon between the atmosphere and biosphere. Photosynthesis by plants and phytoplankton as well as respiration by plants and animals including microbes are the two main components of the fast, biological carbon cycle. During photosynthesis, sugars are formed from CO_2 and water with photosynthetically active radiation (PAR), resulting in the release of oxygen. During respiration, sugars are broken down to release oxygen, a process which releases energy, CO_2, and water. Carbon dioxide released from these reactions is usually ending up back in the atmosphere (Riebeek 2011). Each year approximately 120 Gt of carbon is released back into the atmosphere through ecosystem respiration (Luo and Zhou 2006). Globally, terrestrial ecosystems currently remove more carbon from the atmosphere than they release. A net sink of approximately 1.9 (± 1.1) Gt yr^{-1} is recorded (IPCC 2022). However, some ecosystems particularly northern ecosystems including Arctic ones, which warm faster, have been shifted from net carbon sinks to net carbon sources due to climate change (Virkkala et al. 2021).

2.2.2 Slow carbon cycle

Slow C cycle moves carbon between rocks, oceans, soils, and atmosphere and it takes hundreds to thousands of years to complete. Summarized by Riebeek et al. (2011) the slow C cycle, sometimes also called the chemical carbon cycle, begins when atmospheric C combines with water to form carbonic acid. Via chemical weathering carbonic acid dissolves rocks and releases ions such as calcium, magnesium, or sodium. When these ions react with carbonic acids dissolved in the water carbonates are formed. These carbonates are then deposited on the ocean floor and with time form limestone and its derivatives. Carbon can also be formed into rocks from organic carbon, thereby linking the slow C cycle with the fast C cycle. Sedimentary rocks, e.g., shales, are formed when organic carbon is compressed with heat and pressure over millions of years. Apart from sedimentary rocks, organic matter can also form oil, coal, or natural gases. This occurs when dead organic matter builds up more rapidly than it can decay (Riebeek 2011).

In addition, the slow carbon cycle also includes carbon reactions in oceans. At the water surface, CO_2 dissolves in and ventilates out of the water in exchange with the atmosphere. When CO_2 dissolves into the ocean it reacts with water molecules and releases hydrogen making the oceans more acidic. Hydrogen reacts with carbonate and produces bicarbonate ions. Before the industrial age, the carbon ventilation out of the ocean and the carbon the ocean received via rock weathering used to be in balance. Since then, the oceans now take up more carbon than they release, due to the increasing atmospheric CO_2 concentrations (Riebeek 2011).

2.2.3 Human impact on carbon cycles

Humans have caused a major disturbance in the slow carbon cycle by combusting fossil fuels and harnessing ecosystems for our own use. Billions of tons of carbon that naturally used to be in the slow cycle are now moved to the fast cycle. For example, volcanos emit less than 1 billion tons C into the atmosphere while human activities emit at least 60 times more (Scott and Lindsey 2016). The burning of fossil fuels is the main cause of the rapid increase in atmospheric carbon concentrations. The amount of carbon added to the atmosphere via fossil fuels might seem

small in comparison to the gross fluxes from natural fast processes, e.g., photosynthesis and respiration. However, these fluxes are large in comparison to the natural net carbon fluxes. The land biosphere and ocean together remove about 4 Pg of carbon each year, while out of the 7 Pg C which is blown into the atmosphere every year by fossil fuel emissions, about 3 Pg C remains in the atmosphere (Kondo et al. 2020). That shows that the human contribution to the atmospheric CO_2 concentration is undeniably huge. The rise in atmospheric CO_2 concentration causes global warming, which is connected to the central question of this thesis: what are the consequences of global warming on soil carbon fluxes?

2.3 Soil CO_2 fluxes

Globally soil contains over 3 000 Pg of carbon. Most of the soil carbon is stored in wetlands (450 Pg (Nahlik and Fennessy 2016) and in permafrost soils (1200 Pg) (Hugelius et al. 2014). The amount of carbon in soils is over three times higher than the amount of carbon bound in the aboveground biomass (650 Pg) (Luo and Zhou 2006). The total sum of plant and soil carbon pools (3800 Pg) is five times higher than the size of the atmospheric pool (750 Pg) (Luo and Zhou 2006). Soils in the northern latitudes are significant carbon stocks. Even though northern high-latitude soils cover only 5 % of the terrestrial global surface, they store 30 % of the global carbon (Sigurdsson et al. 2016). The build-up of organic matter in the northern latitudes is due to cold conditions, slow decomposition, a large number of waterlogged regions and the high amount of C preserved in the permafrost that is not part of the active C cycle but is at risk of being released (Sigurdsson et al. 2016; Hugelius et al. 2014).

Both, fast and slow C cycling processes are present in soils. A significant part of the fast carbon processes occurs in soils (Kutsch et al. 2009). Decomposition, where dead plant materials are used by the microbial community is a key component in the soil carbon cycle. Soil organic matter (SOM) concludes the living and dead biomass of microbes, plants, and fauna. Soil organic matter is a significant store of carbon. Carbon can be stored in the soil for even thousands of years before it's used in microbial respiration and broken back down to CO_2 (Kutsch et al. 2009). Soil respiration is described as follows by Luo and Zhou (2006). Both plant respiration (R_p) and soil

microbial respiration (R_m) release CO_2 back into the atmosphere. Plant respiration can be divided into aboveground respiration (R_a) and below-ground plant respiration (R_b). Below-ground plant respiration occurs via root respiration, which includes also rhizomicrobial respiration. Root respiration generally accounts for approximately 50 % of the total soil respiration (R_e) (Kutsch et al. 2009). Plant respiration can be described as autotrophic respiration and R_m as heterotrophic respiration (Luo and Zhou 2006). Carbon processes are illustrated in Figure 1.

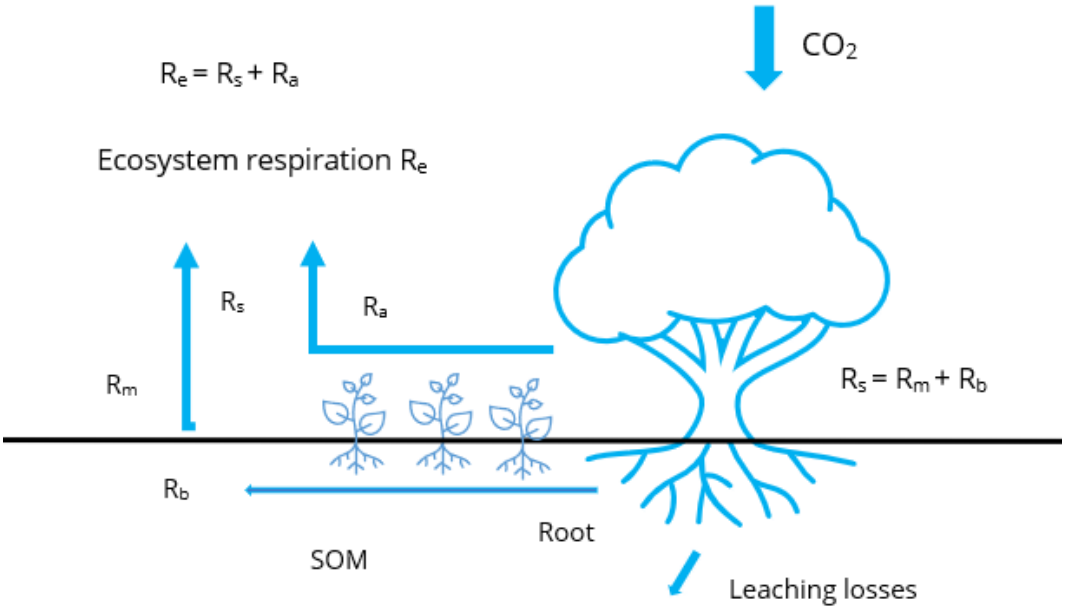

Figure 1 Schematic diagram of ecosystem carbon processes. Plants take up CO_2, which is then further used by the microbial community in decomposition and released back into the atmosphere via soil respiration. Together with aboveground vegetation-mediated respiration soil respiration forms the total ecosystem respiration. Abbreviations: R_e = total soil respiration, R_s = soil respiration, R_a = aboveground respiration, R_m = microbial respiration, and R_b = below-ground respiration.

2.3.1 Biological CO_2 production

CO_2 is released from soils into the atmosphere via soil respiration as described above. It is a key process in soil carbon cycling and represents the second-largest carbon flux between terrestrial ecosystems and the atmosphere. CO_2 is produced through many biochemical pathways. The most common of these is the tricarboxylic acid (TCA) cycle, also known as the Krebs cycle, which

is the main source of energy for all cells (Luo and Zhou 2006). In TCA, energy is created by oxidizing sugars in aerobic conditions. CO_2 can also be produced in several anaerobic respiration processes during fermentation. (Luo and Zhou 2006). Given the large magnitude of C stocks residing in the soil, even small changes in soil respiration can have significant effects on CO_2 concentrations in the atmosphere.

2.3.2 Abiotic CO_2 production

Apart from biological soil carbon production, carbon can also be produced abiotically. Inorganic soil carbon mainly consists of carbonates such as calcite, aragonite, dolomite, and siderite (Lal 2007). As explained in chapter 2.2.2, these carbonates are formed in weathering or when soil minerals react with atmospheric CO_2. Naturally abiotic carbon is returned to the atmosphere along volcanoes or via other geothermal activity, which is addressed in this thesis. Globally, during a ten-year time period CO_2 flux from volcanoes was estimated to be around 51.3 Tg CO_2 y^{-1} for non-eruptive emissions, and around 1.8 Tg y^{-1} for eruptive emissions (Fischer et al. 2019).

2.3.3 Transport of CO_2 from soils and controlling factors

Carbon dioxide produced in soils through biological and chemical processes leads to soil CO_2 concentrations which are typically much larger in soil than in the atmosphere. Diffusion is the main mechanism of CO_2 release from the soils (Luo and Zhou 2006). Gaseous CO_2 transport is mainly driven by the concentration gradient along the soil from deep layers to the soil surface. The CO_2 concentration is generally relatively lower near the soil surface as compared to the deep soil layers. This gradient develops even though CO_2 is produced more in the surface layers than in the deep layers, due to CO_2 release into the atmosphere. One other reason is that CO_2 has a natural tendency to sink in the soil and that CO_2 accumulates in deeper soil layers due to the compaction of the soil (Luo and Zhou 2006).

Both abiotic and biotic factors regulate CO_2 fluxes from the soil. The major factors are substrate supply, temperature, moisture, oxygen, carbon and nitrogen content, soil texture, and pH (Luo

and Zhou 2006). The influence of temperature, moisture, and soil carbon on CO_2 production and fluxes are described more specifically in the following chapters.

Temperature affects almost every aspect of the respiratory process (Luo and Zhou 2006). It has been shown that soil warming can stimulate decompositions by enhancing the decomposition rates and therefore increase microbial CO_2 production (Lei et al. 2021; Romero-Olivares et al. 2017). In a meta-analysis by Romero-Olivares et al. (2017), the temperature was shown to increase soil respiration and C losses from soils in a short time (≤ 4 years) but caused a decrease in soil respiration over a longer period (> 10 years). However, temperature effects were not found to be significant for fungal biomass, microbial biomass, or microbial carbon in the long term. The acclimation of soil microbes, evolutionary adaption, shifts in the microbial community, or depletion of labile C was suggested to be the driving factors for the diminishing warming effects over time. This meta-analysis was performed with 25 field experiments from 11 different types of ecosystems, including e.g., alpine grasslands, boreal forests, and tundra. These experiments lasted from 1 to 15 years. However, more long-term studies are needed to achieve a robust idea of the temperature effects because observed short-term soil C losses might be much greater than the actual long-term losses (Romero-Olivares et al. 2017).

Soil carbon content and temperature have significant combined effects on soil respiration. Lei et al. (2021) stated that although there is an ongoing debate, earlier warming experiments indicate that warming-induced soil C losses might be associated with the standing soil C stock. Meaning that more C losses occur in soils with higher C stocks (Lei et al. 2021). They proved that the temperature effects on R_s rates are correlating with soil organic carbon (SOC). Negative R_s rates were shown to occur especially in the grasslands and mixed forests with low SOC stocks and positive R_s rates in the evergreen forest with high SOC stocks (Lei et al. 2021).

In addition, soil moisture is another main factor that influences respiration. Soil moisture affects respiration directly via physiological processes of micro-organisms and roots, and indirectly through the diffusion of CO_2 and substrates (Luo and Zhou 2006). The general perception is that CO_2 fluxes are low in dry soils, reaching the maximal rate in intermediate moisture levels, and

decreased in high moisture levels when anaerobic conditions decrease aerobic microbial activity (Luo and Zhou 2006). The optimum is usually when the macropore space is mainly air-filled and the micropore space is mainly water-filled, around 60 % of water-filled total pore space (Luo and Zhou 2006). High soil moisture content correlates with low air-filled pore space and when soil moisture conditions are high oxygen concentration is usually the primary regulating factor (Luo and Zhou 2006).

2.4 Soil CH_4 fluxes

Methane is produced in soils both abiotically and biotically, in aerobic and pre-dominantly anaerobic conditions. It has been stated that the main natural sources of methane are biological processes in anoxic environments conducted by methanogens (Serrano-Silva et al. 2014).

2.4.1 Biological CH_4 production

Methanogens are microbes, both archaea, and bacteria, that produce methane (Serrano-Silva et al. 2014). Anaerobic archaea are the main producers of CH_4 in soils (Serrano-Silva et al. 2014). Methane production occurs with low redox potential when chemical agents such as molecular oxygen, nitrate, or iron (III), with high redox potential have been thoroughly reduced (Serrano-Silva et al. 2014). These conditions are often found when prolonged water logging is present e.g., in flooded rice fields, wetlands, and sediments (Serrano-Silva et al. 2014). Methane production can be observed as a four-step process: 1) hydrolysis of macromolecules and polymers, 2) acidogenesis, 3) acetogenesis, and 4) methanogenesis by archaea. Methanogenesis only occurs in microbial communities where other organisms producing suitable substrates such as acetate and hydrogen are present. (Serrano-Silva et al. 2014).

2.4.2 Abiotic CH4 production

In addition, methane production has been measured in oxic soil samples collected near plants (Serrano-Silva et al. 2014). The role of abiotic formation of CH_4 with highly oxidative ambient conditions has been contemplated to have possible significance in soils (Serrano-Silva et al. 2014). CH_4 fluxes have been measured from soil temperatures that exceed the limits of known enzymatic activity of methanogens (> 70 °C) (Serrano-Silva et al. 2014). This has been considered to show the existence of a chemical CH_4 production process under oxic conditions in soils without directly involving organic matter. However, the reaction pathway is not thoroughly known yet (Serrano-Silva et al. 2014). It has been hypothesized that methanogens are not the sole source of CH_4, and non-microbial formation must be taken into consideration. (von Fischer and Hedin 2007; Althoff et al. 2010; Kammann et al. 2009). Abiotic CH_4 production can be derived by either high-temperature magmatic processes in volcanic and geothermal areas or temperatures below 100°C in so-called gas-water-rock reactions in continental settings (Etiope and Sherwood Lollar 2013). Fischer-Tropsch Type (FTT) reactions, e.g., the Sabatier synthesis between H_2 and CO_2, are suggested to be the main source of abiotic CH_4 in natural conditions (Etiope and Sherwood Lollar 2013). It is generally considered that abiotic methane is mainly released into the atmosphere via magmatic processes. However, gas-water-rock reactions have also been shown to be more prevalent than thought earlier (Etiope and Sherwood Lollar 2013).

2.4.3 Transport of CH_4 from soils and controlling factors

Main CH_4 emissions from soils to the atmosphere consist of three possible mechanisms. 1. diffusion of gaseous methane through the soil profile along a concentration gradient as described above for CO_2, 2. ebullition (release of gas bubbles), and 3. trough aerenchyma of vascular plants.eg., *Carex*. Diffusion is slower than ebullition or plant-mediated transport, but it has great importance in the total net CH_4 emissions (Serrano-Silva et al. 2014). The CH_4 production in the soil doesn't equal the total CH_4 emissions. This is because methanotrophic bacteria use CH_4 as a C and energy source and oxidize CH_4 in the upper aerobic soil layer, thereby reducing the total amount of CH_4 emitted to the atmosphere (Serrano-Silva et al. 2014).

There can be even net uptake of CH_4 from the atmosphere, causing a negative flux of CH_4 from the atmosphere to the soil (Maljanen et al. 2018). Carbon dioxide is generated when methanotrophs oxidize CH_4. (Luo and Zhou 2006). It is considered that up to 80 % of CH_4 produced by methanogenic archaea is consumed by methanotrophic bacteria at the soil surface (Serrano-Silva et al. 2014). Methanotrophs can survive in different environments. For example, methanotrophic psychrophiles can grow in very low temperatures and play an important role in the CH_4 balance in permafrost soils and the northern taiga and tundra. (Serrano-Silva et al. 2014).

Several environmental factors affect the population of methanotrophs, most significantly temperature, pH, N sources, and CO_2 and O_2 concentrations. CH_4 oxidizers use O_2 as an electron acceptor and the enzyme initiating the reaction can use both CH_4 and NH_4^+, since the molecules are the same in structure and size (Serrano-Silva et al. 2014). Therefore NH_4^+ fertilizers can inhibit CH_4 oxidation (Serrano-Silva et al. 2014). CH_4 oxidation is considered to decrease when the soil water content increases. The pH range for methanotrophs is wide, from 3.5 up to 9.9. (Serrano-Silva et al. 2014). The considered determining factors for methanogenesis are the availability of organic matter (OM), and the concentration of O_2. Environments rich in sulfate have been shown to inhibit methanogenesis due to the competition from substrates with sulfate-reducers (Serrano-Silva et al. 2014). Methane production and fluxes are closely associated with vegetation. Methanogens use easily degradable root exudates as substrates and as mentioned above, plants can also transport CH_4 to the atmosphere. Short-term incubation experiments have proven that CH_4 emissions increase with increasing atmospheric CO_2 and temperature (Serrano-Silva et al. 2014). High temperature and CO_2 concentration have been shown to decrease the oxidation of CH_4 and increase methanogenesis (Das and Adhya 2012). All in all, it is estimated that climate change will increase CH_4 emissions from soils. However, long-term studies are still needed also in this area of study to gain more knowledge about the coeffects of temperature, and CO_2, as well as about the possibilities of long-term adaptations of microbes (Serrano-Silva et al. 2014).

2.5 Exchange of CO_2 and CH_4 between atmosphere and soil ecosystem

As described above there are several components that form soil respiration. For example, roots can have a significant impact on the total GHG emission rates (Luo and Zhou 2006). Together all different soil respiration components might have different responses to elevated CO_2 concentrations and temperature. Additionally, they have different impacts on the climate system. While plant respiration can be described as bioenergy, where CO_2 emitted has been recently fixed, CO_2 from soils increases the CO_2 load of the atmosphere. To gain an accurate knowledge of the effects of soil respiration on the global C budget of ecosystems we must be able to study these components separately. The heterotrophic respiration (R_b) and the autotrophic respiration (R_m) are however tightly connected. (Luo and Zhou 2006).

2.5.1 Common chamber methods

Chamber measurements are the most widely used method for soil respiration measurements (Subke et al. 2021). There are two types of chamber measurements, static and dynamic (Luo and Zhou 2006). Chambers should be opaque, to prevent any light from penetrating and thus CO_2 uptake through photosynthesis. In the dynamic chamber measurements, air moves between the chamber and a gas analyzer. An infrared gas analyzer (IRGA) is the most commonly used sensor in dynamic chamber measurements to detect CO_2 fluxes (Subke et al. 2021). In the closed dynamic chamber method, changes in the CO_2 concentrations in the chamber are measured over a short time (ca. 5 minutes) (Hutchinson et al. 2000). CO_2 concentrations can also be measured from an open dynamic chamber, where differential changes in CO_2 are measured in a continuously ventilated state. In the closed static chamber measurements, CO_2 is trapped in an alkali solution or soda lime (Luo and Zhou 2006). Static chambers can also be used to measure concentrations during enclosure with syringe samples. These samples are then analyzed with a gas chromatograph (GC) or IRGA. (Luo and Zhou 2006).

In closed chamber measurements CO_2 concentrations in the chamber increase over time. To determine the CO_2 efflux, several data points are needed during the measurement. The respiration rate can then be calculated with a linear regression equation. In addition, a non-

linear regression equation is also applied because concentration gradients are altered with the build-up of CO_2 in the chambers. (Luo and Zhou 2006). Approaches described above have been most widely used and studied with CO_2, but the basics of each chamber method also apply to other GHGs such as CH_4. When measuring CH_4 a longer sampling time is typically required due to the lower mixing ratio and CH_4 concentrations in the atmosphere and thus slower changes in the concentrations per mass unit compared to CO_2.

2.5.2 Soil gas gradient method

The soil gas gradient method can be used to calculate the gas flux based on concentration measurements from porous media when assuming that diffusion is the main transport mechanism (Maier and Schack-Kirchner 2014). The gradient method is based on the soil gas diffusivity, soil structure, and soil profile gas concentrations. Soil gas diffusivity has to be first estimated using e.g., models, in situ approaches such as the so-called Radon method or laboratory measurements (Maier and Schack-Kirchner 2014). The flux can then be calculated using a variety of approaches from very simple direct calculations to high analytical equations. E.g., linear regression or concentration calculation of various points and extrapolating the flux between them can be used for flux calculations. There are several limitations to the method such as low concentration change, high wind seed and wet soils where diffusion is limited (Maier and Schack-Kirchner 2014). The gradient method works best when gas exchange only occurs via diffusion. It is ideally applied only in horizontally homogeneous and well well-aerated soils (Maier and Schack-Kirchner 2014).

2.5.3 Other methods for CO_2 and CH_4 flux measurements

Additionally, today there are several portable as well as automated in situ devices that measure both CO_2 and CH_4 concentrations directly in real-time e.g., Li-Cor laser-based Trace Gas Analyzer (Li-Cor 2022). The micrometeorological eddy covariance (EC) method is one of the most commonly used methods. EC typically provides direct flux rates of water, energy, and GHGs at the ecosystem scale. With EC it is possible to achieve high temporal resolution (i.e., hourly fluxes) based on concentration measurements at 10-20 Hz (Monteith and Unsworth 2013; Helsingin

yliopisto 2013). The main advantaged of EC compared to chamber methods is the high-temporal resolution when chamber methods have a comparatively high spatial resolution (Monteith and Unsworth 2013; Hutchinson et al. 2000).

2.5.4 Trenching method

Trenching is the simplest and most commonly used method to separate root respiration from microbial respiration (Kutsch et al. 2009). In trenched plots, all parts of plants have been cut from the soil surface. Trenched plots vary in size and depth according to the study site's characteristics. The most common technique is digging a large trench around the plot, lining it, and then filling it again. E.g., plastic materials or landscape fabric can be used as a lining material (Kutsch et al. 2009).

Even though trenching is an efficient technique for measuring soil microbial respiration it has several limitations. It has been shown that after trenching the respiration rates increase (Kutsch et al. 2009). A significant part of heterotrophic respiration is derived from newly produced material such as decaying roots. In trenching experiments, this input decreases. It is not fully clear when the dead roots cease respiring, and the respiration can be considered heterotrophic (Kutsch et al. 2009). Trenching can also affect other conditions of the soil, especially the water content might be increased due to the eliminated plant uptake. Additionally, it has been shown that root exclusion affects microbial biomass and nitrogen dynamics (Kutsch et al. 2009). There are also stable isotope methods, but they are cost-intensive and can only be applied to systems where the plants and the soil carry a different isotopic signature, which is rare (Kuzyakov 2006).

2.6 Warming experiments to study temperature sensitivity of CO_2 and CH_4 exchange

Warming experiments play a key role when we want to gain a deeper understanding of ecosystem vulnerability in changing environments. Warming experiments can be conducted with multiple approaches, each having shortcomings and advantages. Logistical and financial

obstacles are often limiting these studies. Warming experiments can be done either in laboratories or in the field. Microcosms in the laboratory can provide detailed information about the mechanistic drivers of the temperature effects, but large-scale ecosystem complexity is impossible to achieve in the laboratory setup (O'Gorman et al. 2014; Sigurdsson et al. 2016). In situ methods, open-top chambers (OTC), transect studies, and natural warming gradients are the most common approaches used in warming experiments (Hollister et al. 2022; O'Gorman et al. 2014; Sigurdsson et al. 2016).

Artificial warming is usually conducted with tents, chambers, or greenhouses of various sizes and shapes. In OTCs, gases are in exchange with the atmosphere and precipitation can enter the plot. OTCs were already used broadly in the 1980s (Hollister et al. 2022). Warming with OTCs can be conducted either passively or actively. In actively warmed chambers heated air is conducted with a fan through the chamber. OTC measurements have been criticized for the large variability in the temperatures between controls and treatment chambers (Aronson and McNulty 2009). Solar radiation angle and the weather conditions such as cloudiness also affect the warming rate of the chamber (Hollister et al. 2022). Other active warming methods, especially in ecological studies are e.g., overhead IR lamps and heat resistance cables (De Frenne et al. 2013; Aronson and McNulty 2009). One advance in warming experiments described above is that it is possible to study warming effects even in the very extreme predicted temperatures or patterns that are not yet occurring in specific ecosystems (de Frenne et al. 2013).

The importance of long-term ecological studies is vital, and they are needed to gain a robust idea of the effects of warming. Transect studies can provide low-cost long-term insight into warming effects (de Frenne et al. 2013). Transect studies such as comparing altitudinal and latitudinal gradients offer an approach focusing more on large-scale ecosystem structure and functioning, compared to the experimental warming methods (de Frenne et al. 2013). Transect studies have been criticized for the confounding impacts that can occur in a single transect (e.g., change in soil and vegetation type) and can be mistaken for a climate signal (Caddy-Retalic et al. 2017; de Frenne et al. 2013).

In addition to transect studies, naturally warmed ecosystems provide a low-cost approach compared to artificial warming methods (O'Gorman et al. 2014). Naturally warmed ecosystems are warmed via geothermal activity and offer a possibility to study effects on long temporal scales, within smaller spatial scales where soil and vegetation types do not change (Sigurdsson et al. 2016). In these areas, a wide range of temperatures can be found within a sole biogeographic area. Geothermally active regions can be found especially around the edges of tectonic plates. They are warmed via the heated water accumulating under an impermeable rock with high pressure. Warming has usually occurred over a long period in naturally warmed regions and is therefore suitable for studying long-term evolutionary and ecological responses (Sigurdsson et al. 2016; O'Gorman et al. 2014). Geothermal ecosystems can be considered as an ideal platform for performing multi-scaled research and for helping to gain valuable information on the complex ecological responses to warming (O'Gorman et al. 2014). However, there are also several limitations to geothermal gradients. One of them is that in these sites only the soil is warmed rather than the air, which is the major factor in global climate warming. Another difference from gradual climate change is that geothermal warming generally starts with a phased change in soil temperature.

2.6.1 Natural warming studies in Iceland and ForHot study sites

Iceland is famous for its geothermal activity and several natural in situ warming experiments have been carried out there. These study sites in Iceland have already revealed a piece of valuable information e.g., on temperature effects on community composition, population abundance, ecosystem functioning, and food web structures. (O'Gorman et al. 2014).

A major earthquake (6.3 M_L) occurred in southwest Iceland in 2008. The earthquake affected the geothermal system close to the epicenter by moving it to a new location. The area wasn't previously warmed but after the earthquake soil temperatures significantly increased. New belowground geothermal channels increased soil temperature varying from + 0°C up to + 52°C (ForHot 2021). The warmest areas occur where the channels are closest to the surface. This made it possible to study long-term warming effects with different temperature increases on the previously unwarmed area. Furthermore, two different types of ecosystems, forest, and

grassland offer a unique opportunity to also compare the effects between ecosystems (ForHot 2021).

ForHot research network was established after the 2008 earthquake to study the temperature effects in these areas in natural soil warming experiments. ForHot is coordinated by the Agricultural University of Iceland and there are already over 70 papers published by the community. (ForHot 2021). There are three main study sites in the use of the Forhot researchers: newly planted forest (FN), new grassland (GN), and older grassland (GO). FN (forest new) is a Sitka Spruce Forest (*Picea sitchensis*). There are naturally only a few forests in Iceland. The FN Forest was planted between 1966 and 1967. GN is dominated by the grass *Agrostis capillaris,* some herbs and mosses. These sites are located in Southern-Iceland near the village of Hveragerð. The third site is located approximately 2 km northwest of FN, and GN. GO is an older geothermal gradient where the first survey of geothermal hot spots was made already in the 60s. (ForHot 2021; Sigurdsson et al. 2016).

2.7 Volcanic areas

In addition to biologically mediated CO_2 and CH_4 volcanic areas can also emit geological CO_2 and CH_4 making it more complicated to study in situ soil respiration. These abiotic CO_2 and CH_4 fluxes have been unveiled to be more dominant in high temperature geothermal areas, than the parallel biogenic gases. (Maljanen et al. 2020; Tassi et al. 2015). Volcanic CO_2 is mainly of magmatic origin (Ármannsson 2018). CH_4 emitted from geothermal systems has been suggested to be predominantly generated by abiotic reduction of CO or CO_2 (Tassi et al. 2015).

Besides CO_2 and CH_4 concentration measurements, non-biogenic and biogenic CO_2 and CH_4 must be separated to be able to study the temperature responses of soil respiration. Stable isotope approaches, described below, can be used to disentangle these sources. It should be noted, however, that even when we talk about biogenic and geological emissions, the carbon in both thermogenic and bacterial gases, has been part of the biological cycle of the exogenic carbon processes (Whiticar 1999).

2.8 Basics of stable isotope approach

Stable isotope approaches have been applied in various studies in the fields of chemistry, ecology, geochemistry, and biogeochemistry. The ratio of the heavier isotope or in other words the rarer isotope to the lighter, more common isotope is the key in isotope analyses. In natural conditions, the heavier isotope usually fractionates in chemical reactions. More energy is needed to break down the bonds in molecules that contain the heavier isotope because of the lower potential energy compared to the lighter element. As an outcome, the abundance of the heavier isotope in the product is smaller than its abundance in the substrate. This fractioning makes it possible to gain valuable information about elements cycling in the environment. The fractionating can be divided into kinetic fractionation and equilibrium fractionation. Kinetic fractionation means that the reactions are dependent on the mass and that the reaction is unidirectional. In equilibrium fractionation, the isotope distribution is the same in back-and-forth reactions. These reactions are rarely ever completed and occur in closed systems. (Peterson and Fry 1987; Dawson and Siegwolf 2007).

The δ notation is applied to represent the difference in isotope abundances relative to an international standard. The δ-value is calculated with Equation 1, where XX is the atomic mass of the heavier isotope in the ratio, E is the studied element, R is the absolute ratio, SA is the sample, and STD is the internally accepted standard.

Equation 1

$$\delta^{XX}E = \frac{R_{SA}}{R_{STD^{-1}}}\ x\ 1000$$

The unit of the δ notation is ‰. The standard δ-value is 0 ‰, meaning that if the sample has a more negative δ-value it is enriched with the lighter isotope, and vice versa if it is positive the sample is enriched with the heavier isotope. The standards are determined by the International Atomic Energy Agency (IAEA). (Dawson and Siegwolf 2007).

2.8.1 Use of stable isotopes in studies of CO_2 and CH_4 fluxes from ecosystems

The isotope signal of CO_2 and CH_4 from biological respiration differs from CO_2 and CH_4 derived from geothermal sources. These gases from the geothermal fields in Iceland are significantly enriched in ^{13}C compared to other carbon sources such as the CO_2 from the atmosphere. The Keeling plot approach (Keeling 1958; Maljanen et al. 2020) can be used for calculating the $\delta^{13}C$ values of CO_2 or CH_4 emitted from the surface. The Keeling plot method is based on the regression of the $\delta^{13}C$ and mixing ratios relative to the background air values. It can be calculated by plotting the concentrations of the wanted gas against the measured $\delta^{13}C$ values and calculating the intercept. This intercept represents the keeling plot and furthermore the accurate $\delta^{13}C$ value. With the isotope mixing model, it is feasible to determine the different sources' proportions of the isotopes. When defining the sources with stable isotopes the source δ-values must be repeatable and distinct. These are called the end members of the isotope mixing model. The only way to separate biotic and abiotic fluxes is to implement the isotope technique, as described above. With a two-pool isotope mixing model, the abiotic and biotic sources of CO_2 can be defined. (Majlesi et al. 2020; Maljanen et al. 2020) The mixing model is presented in Equation 2.

Equation 2

$$f_1 = \frac{(\delta - \delta_0)}{(\delta_1 - \delta_0)}$$

Where δ is the isotopic signature of CO_2, δ_0 is the isotopic signature of the geothermal source and δ_1 stands for the biological source. F_1 is the fraction of the geological source. Biological fraction (F_2) can be calculated by subtracting F_1 from 1 and multiplying it with 100 to obtain the percentual fraction.

3 Objectives

The main aim of this study is to investigate the effects of natural soil warming on soil microbial respiration rates in a subarctic spruce forest. The goal is to gain valuable information on the responses of soil decomposition processes to medium-term natural warming and provide more insights into mechanisms underlying the responses. This study aims to identify the sources of CO_2 fluxes, by firstly eliminating the effects of vegetation by removing the roots from the soil samples, secondly partitioning the CO_2 fluxes with isotope approaches, and finally accurately determine the temperature sensitivity of biological respiration. In addition to CO_2 fluxes, temperature effects on CH_4 fluxes are studied.

4 Material and methods

4.1 Study site

The sampling was conducted at the subarctic ForHot FN site (64.008°N, 21.178°W). The FN site is divided into six temperature transects from A to F. Figure 2 shows the FN site *Sitka Spruce* Forest and the 6 temperature transects. There are five sampling plots in each transect. A-plots (blue) are the ambient temperature plots, B plots +2°C, C plots +6°C, D plots +10°C, E plots +20°C, and F-plots (red) are the warmest plots, warming up to +40 °C (Sigurdsson et al. 2016). These temperatures are measured in 10 cm depth. The FN Forest has been planted with Sitka spruce (*Picea sitchensis*) in 1966 and has never been thinned (Sigurdsson et al. 2016). It has a relatively high density compared to a typical Icelandic spruce forest (Sigurdsson et al. 2016; Maljanen et al. 2020). The mean annual temperature in the study area is 5.3 °C and the mean annual precipitation is approximately 1600 mm (Sigurðsson et al. 2019). The growing season generally starts in May and ends in August (Sigurdsson et al. 2016). During winters there is no permanent snow cover, but the soil can freeze for several months in mid-winter. The soil type is volcanic Andosol, and the texture is silty loam. The three most dominant vascular plant species, apart from the trees, in the study site are *Equisetum arvense, Agrostis capillaris, and Geranium sylvaticum* which grow in the understory (Sigurdsson et al. 2016).

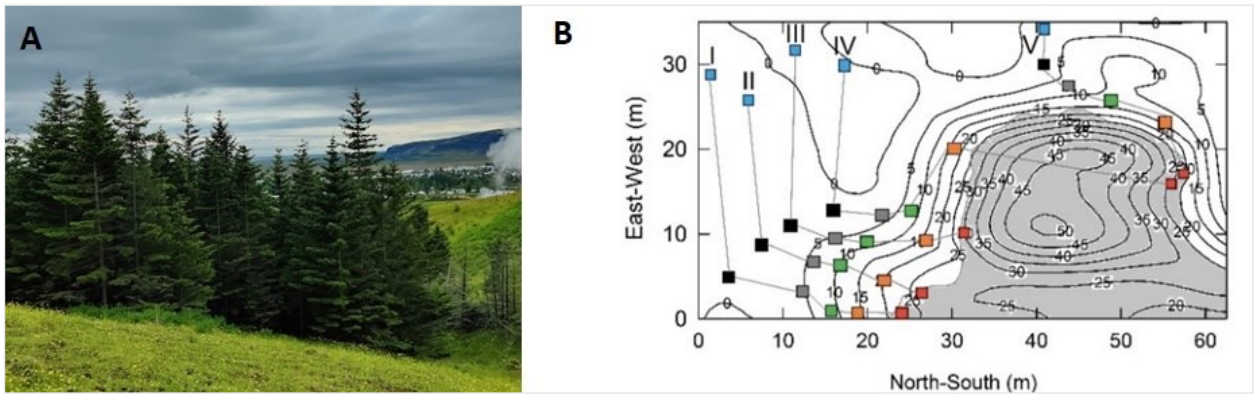

Figure 1 a) FN Sitka spruce forest. b) Temperature transects from A to F and study plots (Sigurdsson et al. 2016). The transects reflect gradually warmed soils due to geothermal activity. Five plots in each transect are coloured *according to the temperature increase.*

4.2 Sampling

All the sampling and measurements were carried out between 14. - 26.7.2022. To be able to measure the R_m rate the roots were cut by trenching the study plots. The trenching was done before the sampling in the previous summer of 2021. Trenching was established by digging a trench of about 10 cm width and 30 cm depth from approximately one square meter area, inserting a geofabric used for gardening, placing the soil back within the 10 cm trench and removing all the aboveground vegetation within the 1x1 m area. The fabric prevents roots from outside to grow into the plot but allows water to flow in both directions. Before measurements, chamber collars (11 cm Ø, 15 cm deep) were inserted into the middle of the trenched plot, where aboveground plants were more frequently removed. A trenched study plot is presented in Figure 3.

4.2.1 Surface CO_2 and CH_4 fluxes

Surface CO_2 and CH_4 fluxes were measured from five trenched plots within each temperature transect from A to F by using an opaque chamber (volume 4.45 l). Concentrations were measured with the LiCor gas analyzer with cavity ringdown technique (LI-7810 $CH_4/CO_2/H_2O$ Trace Gas Analyzer, LI-COR Biotechnology, Lincoln, NE, USA) for 15 minutes in each plot. The long closure time was applied to ensure sufficient increase or decrease in CH_4 concentrations with expected small CH_4 fluxes. Negative CH_4 fluxes were considered as uptake and positive fluxes as emissions to the atmosphere. In addition to the trenched plots, measurements were also done next to the trenched plots in the non-trenched area, by inserting the chamber collar into the soil before the measurements. This was done to compare CH_4 and CO_2 fluxes between trenched and non-trenched plots. Non-trenched plots were measured from the transects A, D, and F with three replicates each (plots 1-3). Collar height was measured in each plot for volume calculations. In total there were 39 replicates for surface CO_2 and CH_4 flux measurements. The remaining aboveground plant parts were removed from the trenched plots before the measurement. The weather was mainly sunny, and no rain episodes occurred during the flux measurements.

4.2.2 Surface fluxes for δ ^{13}C of CO_2 and CH_4

In addition to in situ flux measurements, samples for isotopic signatures of CO_2 and CH_4 were collected with the static closed chamber method (Biasi et al. 2008). Samples were taken from each transect and all five replicates from the trenched plots. Sampling was done by inserting and sealing the chamber to the collar prior to the measurement and sampling 25 ml gas every 2,10,15, and 20 minutes with a syringe. Chambers had a hole in the top for a capillary line to avoid pressure effects and to fit the sampling tube. The top was sealed with a rubber septum. Samples were injected into 12 ml Labco pre-evacuated screw-cap vials (Labco Exetainer®, Labco Ltd., Lampeter, UK), and further analysed at UEF (see 4.3.2). Soil temperature was measured simultaneously with a manual thermometer (TM-80N with K-type thermocouple probe, Tenmars Electronics, Taipei City, Taiwan) and a metal probe from 2, 5, 10, 15, and 20 cm depths. Moisture was also measured with a moisture meter ML-3 Thetaprobe connected to a HH2 moisture sensor (Eijkelkamp, Giesbeek, The Netherlands) during the surface flux measurements in three different points of the plot. The chamber design for the stable isotope sampling and the simultaneous measurements are presented in Figure 3.

Figure 3 Trenched study plot while sampling with the static enclosed chamber method.

4.2.3 Soil gas profiles

The same method was used for soil gas gradient sampling as published by Marushchak et al. (2021). Soil gas samples (25 ml) were taken from the soil profile at 5, 10, and 20 cm depths. Gas profile sampling was performed in transects A, D, and F from three non-trenched plots from each transect. Two replicates were taken in each depth in every plot, and one for analysis of CO_2 and CH_4 concentrations, one for analysis of $\delta^{13}C$ values in CO_2 and CH_4. Gas sampling was performed with a stainless-steel sampling probe (ø = 3 mm, l = 40 cm). Samples were injected into pre-evacuated 12 ml Labco screw-cap vials (Labco Exetainer®, Labco Ltd., Lampeter, UK). Soil temperatures at 5, 10, 15, and 20 cm were measured with a metal probe and manual thermometer (TM-80N with a K-type thermocouple probe, Tenmars Electronics, Taipei City, Taiwan) at each sampling time.

4.2.4 Geothermal vents

To determine the $\delta^{13}C$ values of the geothermal source, geothermal gases were sampled on the 25 and 26 of July 2022, from hot spring vents (figure 4) near the study site. A similar method to the one published by Maljanen et al. (2020) was applied. A chamber was used to isolate hot air rising in the hot spring. Air was sucked into the 50 ml syringe through a hole at the top of the chamber. Syringes were let to cool down and then the samples were inserted into the evacuated vials with needles. Gas samples were collected from two different vents. One located near the GO site and the other near the FN site. In total there were 6 replicates for the vents; four replicates from the GO vent and two from the FN vent. Figure 4 presents the sampled vents.

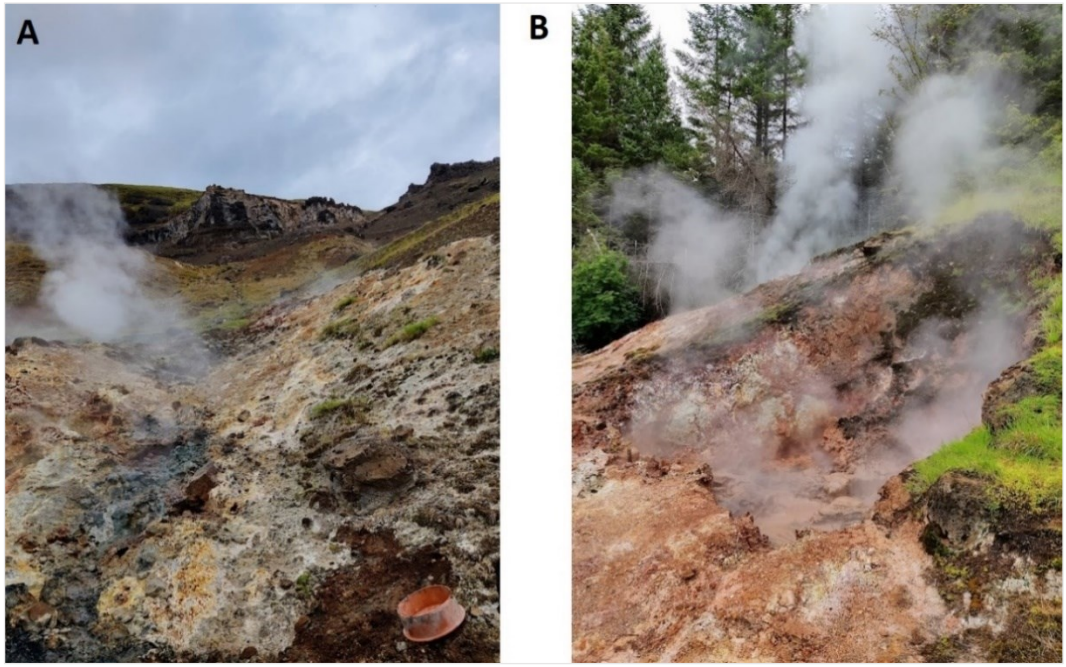

Figure 4 Geothermal vents. A is near the GO study site and B is near the FN site.

4.3 Analyses

4.3.1 Soil and soil water samples

The remaining above ground vegetation was removed and volumetric soil samples were taken with a soil corer (Ø 4 cm) from 0-5 cm depth. They were taken from non-trenched plots in each transect (A-F), three replicates each. Soil samples were processed in Reykjavik in the laboratory managed by the Agricultural University of Iceland and analysed at UEF. First, samples were dried at 60°C for 48 h. The samples were weighed before and after the drying to determine soil water content. Then, a sub-sample of the soil was homogenized with a ball mill to receive a fine powder and homogenize the soil and weighed into tin cups for analysis of %C and $\delta^{13}C$ (2 - 3 mg each) with elemental-analyzer coupled to isotope ratio mass-spectrometer (EA-IRMS). Unfortunately, there were technical problems with the EA-IRMS at Kuopio, UEF, at the time this thesis was carried out and these samples could not be analysed. Thus, the data presented here are %C and $\delta^{13}C$ values from soil sampled in a similar matter a year before this study was conducted (2021). It was assumed that %C and $\delta^{13}C$ values did not change significantly over the

course of a year and can thus be used here. Additionally, root samples were taken from the trenched plots inside the collars with soil corer (Ø 4 cm) from 0-5 cm depth. They were taken from each transect, three replicates each. The roots were separated in the lab with a 1.18 mm sieve and then dried at 60°C for 48 h and weighed. This was done to ensure that roots have decayed since trenching and that root respiration was minimal.

Soil water was collected from lysimeters installed at the site from transects A to E since transect F was too dry for collecting water samples. 40ml of water was collected in each transect. Water was transported to UEF in plastic bottles and frozen until analysed. Total organic carbon (TOC), total carbon (TC), Total inorganic carbon (TIC), and total nitrogen (TN) concentrations were measured with a TOC/TN analyzer (TOC-L/TNM-L, Shimadzu, Kyoto, Japan) from the water samples. Soil water samples were filtered with 0,45 µm syringe filters (Integra Biosciences 153015, Switzerland) before analysis.

4.3.2 Isotopic gas samples

To determine the isotopic values ($\delta^{13}C$) for surface fluxes, soil profiles, and vent samples (CO_2 and CH_4), these gas samples were analysed at UEF with Picarro cavity ringdown spectrometer (G2201-I, Picarro Inc., Santa Clara, CA, USA). The optimal concentration ranges for reliable $\delta^{13}C$ analyses for Picarro were 3 – 100 ppm for CH_4 and 500 – 10 000 ppm for CO_2. To achieve these concentrations samples were diluted based on previous measurements from the site by Maljanen et al. (2020). For surface flux samples with only one replicate, samples from transect F were diluted by inserting 3 ml of the sampled gas into pre-evacuated Labco-vials and diluting it with 22 ml of zero air. For soil profile samples there were two replicates, hence CO_2 and CH_4 were analysed respectively. Samples were diluted from transects D and F. Sample of 18 ml of gas for CH_4 analysis, and 3 ml for CO_2 analysis were inserted in the vials and diluted to the total volume of 25 ml. Certified reference gases, containing 2000 ppm of CO_2, and 10 ppm of CH_4 were also analysed with the samples. Isotope values in the reference gases were – 42.3 ± 0.1‰ for CH_4 and -35.6 δ ± 0‰ for CO_2. There were 3 reference gas samples placed at the beginning and end of each sample run and one after every 15 samples.

4.4 Data processing and calculations

4.4.1 Isotopic gas samples

Samples analysed with Picarro were corrected with actual concentrations and dilution factors. Corrections were done by using Biogeochemistry Research Group's correction script in RStudio (version 2022.7.1.554). The correction effects are shown in the appendixes for ^{13}C of CO_2 and CH_4, and the dilution effect in standards. For CO_2, all results were accepted. For CH_4 all the results that had corrected concentrations over 0.5 ppm were accepted, which is close to the detection limit of the instrument. The $\delta^{13}C$ values were calculated with the Keeling plot method as presented in the literature review (see 2.8.1). All Keeling plots with r^2 higher than 0.80 were accepted.

Against the general Keeling plot assumption, the Keeling plot method was also used for soil gas profiles similar as in Maljanen et al. (2020) to compare the isotopic composition of soil gases with the CO_2 emitted from the surface.

4.4.2 LICOR data

Licor data was processed in MATLAB (version 2022a). The flux calculations were conducted with the Eckhardt and Kutzbach (2016) script. Chamber temperatures measured during the static enclosed chamber measurements for isotopic signals were used for temperature corrections. Temperature change inside the chambers was ca. -0.3 °C for transect A, -0.5 °C for transect B, 0°C for C, -0,2 °C for D, -0.1°C for E, and +4 °C for F during the measurements. The time interval used for flux calculations was 5 minutes. All fluxes were calculated with linear regression. Fluxes with r^2 higher than 0.80 and low RMSE were accepted. For CH_4 if no measurement error was observed, low fluxes (±0.6 mg CH_4 m^{-2} day^{-1}) were accepted regardless of their r^2 value.

4.4.3 Biological and geological fraction

Biological and geological fraction of the total CO_2 flux was calculated with Equation 2, the two-pool isotope mixing model (see 2.8.1). The Keeling plot calculated from the vent samples (-6,98 ‰) was used as the isotopic signature of the geothermal source (δ_0) and the mean value of $\delta^{13}C$ from the A plots (-25,24 ‰) was used as the biological source (δ_1). The $\delta^{13}C$ values of CO_2 and CH_4 from the vents and the $\delta^{13}C$ values of the A plots are presented in Table 1. The average $\delta^{13}C$ values were around -6 for CO_2 and -45 for CH_4.

Table 1 Mean $\delta^{13}C$ of CH_4 and CO_2 in the geothermal vents, mean δ^{13}value of the biological sources of CO_2 measured from transect A and the Standard deviation (SD) and Standard error (SE).

	Mean $\delta^{13}C$	**SD**	**SE**
CO_2 vents	-6.72	0.19	0.14
CO_2 Transect A	-25.24	3.73	1.67
CH_4 vents	-45.26	8.57	6.06

4.5 Statistical analyses

Statistical analyses were performed in RStudio (version 2022.7.1.554). Differences in fluxes between transects were tested with One-Way ANOVA and Tukey's post hoc test. Differences in each transect on biological and geological fluxes were tested with Welch's t-test for non-normally distributed data. Differences in gas concentrations between depths and transects for soil gas profiles were tested with Two-Way ANOVA. Additionally, correlation a matrix (package CORRPLOT, Wei, 2021) was used for the correlations between gas fluxes, soil C content, temperature, and moisture. Results with p-values lower than 0.05 were considered statistically significant, results whit $p < 0.01$ were considered statistically highly significant, and results with $p < 0.1$ were considered marginally significant.

5 Results

5.1 Basic soil characteristics

Measured temperatures from 5 cm (°C), soil moisture (%), carbon content (%C), and $\delta^{13}C$ (‰) values for each transect are presented in Table 2. Soil temperature increased steadily from transect A until transect E. Temperatures measured from transect F (37°C) were higher than in any other transects, representing the extreme temperature increase. Soil moisture and carbon content (%C) decreased in the two warmest transects E and F compared to the other transects. There were no differences in the $\delta^{13}C$ values between transects.

Table 2 Mean measured soil temperatures (°C), soil moisture (%), carbon content (%C), and $\delta^{13}C$ values measured from 0-5 cm soil depth, and SD and SE from transect A-F. The $\delta^{13}C$ values are measured in 2021.

Transect	Mean soil temperature (°C)	Temperature increase (°C)	SD	SE	Mean soil moisture (%)	SD	SE	Mean %C	SD	SE	Mean $\delta^{13}C$ (‰)	SD	SE
A	6.66	+ 0.0	0.54	0.24	55.7	0.87	0.61	11.00	2.53	1.03	-28.41	0.48	0.20
B	6.80	+ 0.2	1.02	0.46	55.5	6.67	3.85	8.31	1.71	0.54	-27.99	0.25	0.10
C	8.10	+ 1.5	0.34	0.15	51.8	2.42	1.40	11.76	1.73	0.71	-28.41	0.25	0.10
D	9.40	+ 2.7	0.95	0.43	57.0	2.51	1.45	10.91	2.28	0.93	-27.87	0.16	0.07
E	11.32	+ 4.7	2.94	1.31	46.8	2.66	1.54	6.91	2.18	0.73	-28.23	0.80	0.28
F	36.56	+ 30.0	4.88	2.18	35.9	4.88	2.82	5.56	1.27	0.47	-27.91	0.91	0.07

5.2 Dissolved C and N content

Total organic carbon (TOC), total inorganic carbon (TIC), total carbon (TC), and total nitrogen (TN) concentrations of soil water samples from the lysimeters are presented in Table 3. Total organic carbon concentrations were highest in transect E with 5.07 mg/L, and lowest in transect A with 3.62 mg/L. Total C and TIC content increased with the increasing temperature with the highest concentrations measured for TC at 65.15 mg/L and for C at 60.29 mg/L from the transect E. Nitrogen content increased with the increasing temperature. The highest TN concentration was measured from transect E with 0.91 mg/L and lowest from the transect A with 0.05 mg/L.

Table 3 Mean TOC, TC, TIC, TN concentrations, and SD and SE for transect A-E.

Transect	Mean TOC (mg/L)	SD	SE	Mean TC (mg/L)	SD	SE	Mean TIC (mg/L)	SD	SE	Mean TN (mg/L)	SD	SE
A	3.62	0.36	0.16	9.74	2.77	1.24	6.13	2.50	1.12	0.05	0.04	0.02
B	3.44	0.75	0.43	10.44	5.80	3.35	7.00	5.06	2.92	0.07	0.02	0.01
C	3.88	0.81	0.40	15.57	10.98	5.49	11.69	10.32	5.16	0.08	0.05	0.02
D	5.07	1.24	0.55	26.40	17.37	7.77	21.32	16.38	7.33	0.20	0.21	0.09
E	4.85	2.31	1.03	65.15	38.96	17.42	60.29	36.74	16.43	0.91	0.61	0.27

5.3 Soil CO_2 fluxes

Carbon dioxide fluxes from non-trenched and trenched plots and the statistical difference between the two plots are presented in Table 4. All CO_2 fluxes were lower in the trenched plots, indicating that the trenching and thus ceasing of root respiration worked. However, the only statistically significant difference (p-value < 0.05) between the trenched and non-trenched plots was measured in transect A (p-value < 0.01).

Overall soil CO_2 fluxes from trenched plots slightly decreased from plots A to B, and then increased steadily to plot E where they reached the highest value of 1258 mg $m^{-2}h^{-1}$. However, flux data from transect E included a large variation. Fluxes were lowest in the warmest transect F with 369 mg $m^{-2}h^{-1}$. There was a significant difference tested with One-Way ANOVA between transects (p = 0.043). Yet, in the pairwise comparison, there were no statistically significant differences between individual transects when tested with Tukey's test.

*Table 4 Means of CO_2 fluxes mg $m^{-2}h^{-1}$ from trenched (n = 23) and non-trenched (n = 10) plots and p-values (** = p < 0.01).*

Transect	Trenched			Non-trenched			Difference
	Mean CO_2 flux (mg $m^{-2}h^{-1}$)	*SD*	*SE*	*Mean CO_2 flux (mg $m^{-2}h^{-1}$)*	*SD*	*SE*	*p-value*
A	468.62	75.06	37.53	765.95	98.62	49.31	0.0060**
B	371.14	126.42	56.54				
C	672.01	291.10	130.10				
D	1009.21	464.26	232.13	1520.31	151.64	87.53	0.12
E	1257.78	756.97	437.04				
F	369.26	206.19	119.04	608.33	41.21	29.14	0.30

5.3.1 The $\delta^{13}C$ values

The $\delta^{13}C$ values for CO_2 from surface fluxes and for both biological (F2) and geological (F1) CO_2 are presented in Figure 5. The $\delta^{13}C$ values increased with increasing temperature and were closer to the geological source in the transect D, E, and F ranging from -11.34 ‰ to -12.93 ‰. Whereas lower $\delta^{13}C$ values measured from the transects A, B, and C were closer to the biological source ranging from -23.00 ‰ to 25.24 ‰.

There was a highly significant difference in $\delta^{13}C$ values between transects with a p-value of 0.0025. In pairwise comparison, there were significant differences between E and A transects (p = 0.038), F and A (p = 0.016), and F and B (p = 0.043). Additionally, a statistically marginal difference was also observed between F and C plots (p = 0.056).

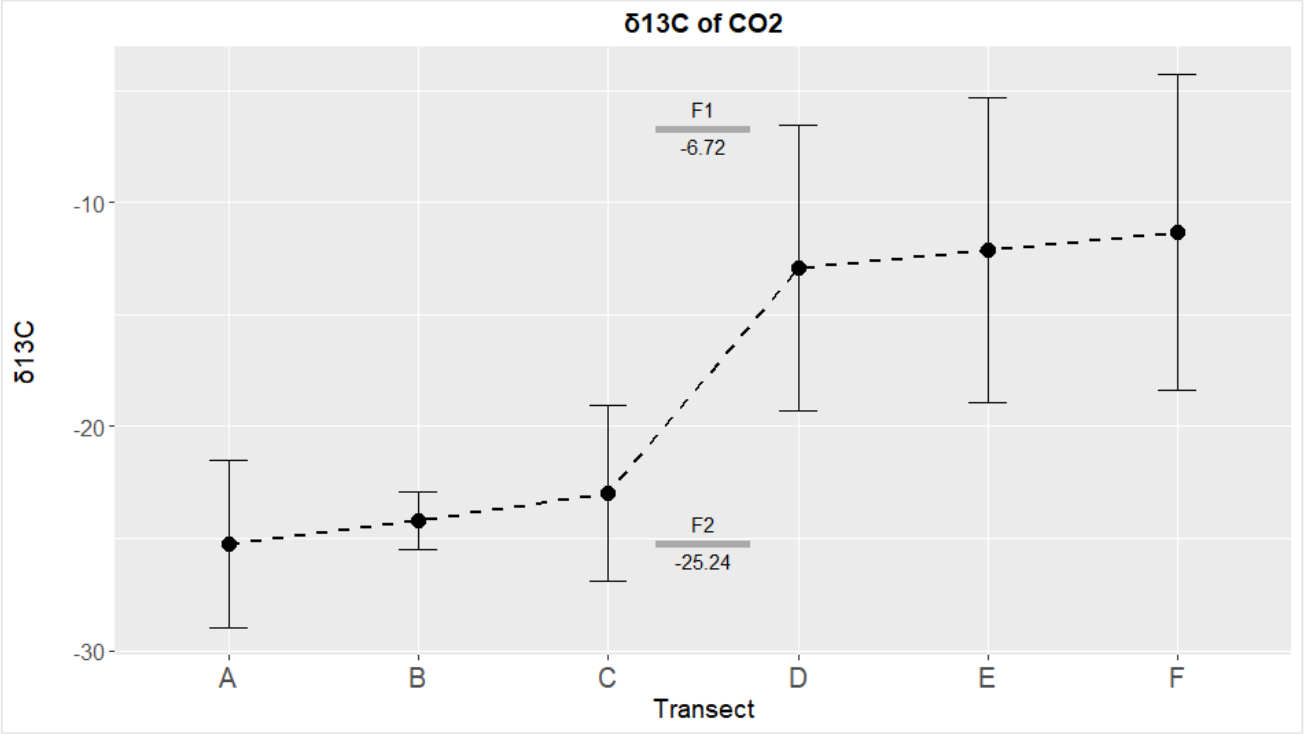

Figure 5 The $\delta^{13}C$ values measured for CO_2 in each transect and the $\delta^{13}C$ values for both biological (F2) and geological (F1) CO_2. The transects reflect gradually warmed soils due to geothermal activity, where A is the ambient temperature and F is the extreme warming (+30°C). The values for F1 and F2 were derived from CO_2 sampled from geothermal vents and surface fluxes from transect A with ambient temperature. Error bars represent the standard deviation.

5.3.2 Fractions of CO_2 fluxes

Figure 6 shows the biological and geological fraction of the total CO_2 emitted, after applying the isotope mixing model. It was assumed that there was no geological flux from transect A, where temperatures were at ambient, and that 100% of the total CO_2 efflux originated from biological respiration. The biological flux component then decreased from transect C to transect E, from 93% to as low as 3%. In transect F, the biological flux component was again higher at 48%. The geological flux component was highest in transect E with 97% of the total CO_2 efflux. The geological fluxes were significantly different between all the transects with a p-value of 0.00416. Significant differences between individual transects for geological fluxes were tested with Tukey's test between transects A and E (p=0.0032), B and E (p=0.0037), C and E (p=0.0036), and F and E (p=0.020). Welch's t-test showed statistical differences between geological and biological fluxes for transects A (p = 0.017), B (p = 0.0049), and C ($p = 2.4* 10^{-6}$). For transect D (p = 0.99), E (p = 0.32) and F (p = 0.54) there was no statistically significant difference between the fraction of biological and geological fluxes. There was only two data point accepted for transect E and three data points accepted for transect F.

After multiplying the biological flux component (F2) with the overall flux, the absolute biological flux was calculated (figure 7). There were highest biological fluxes measured from transect C with a mean value of 520.62 mg CO_2 $m^{-2}h^{-1}$, though this was not statistically different from A, B and D. Lowest biological fluxes were measured from transect E with only 47.83 mg CO_2 $m^{-2}h^{-1}$. When tested with One-Way ANOVA, there was a statistically significant difference in the biological fluxes between all the transects ($p = 2.2 * 10^{-5}$). In Tukey's pairwise comparison, there were highly significant differences shown between transects E and A ($p= 4.4*10^{-4}$), E and B (p= 0.0036), E and C ($p=9.2 *10^{-5}$), F and A ($p= 7.6*10^{-4}$), F and B (p=0.0088), and F and C ($p=1.2*10^{-4}$). Additionally, there were statistically significant differences between E and D transects (p=0.021), and a statistically marginal difference between F and D (p= 0.061).

Figure 8 illustrates the temperature sensitivity of the biological fluxes. There were no clear differences observed rather than a steep decrease in biological flux with extreme temperatures. Correlations calculated with Spearman correlation between the biological flux, C, temperature,

and moisture are presented in Figure 9. There was a negative correlation between temperature and biological flux (-0.39) and also an indication of a strong negative relationship between temperature and moisture (-0.72). Soil %C positively correlated with moisture (0.43).

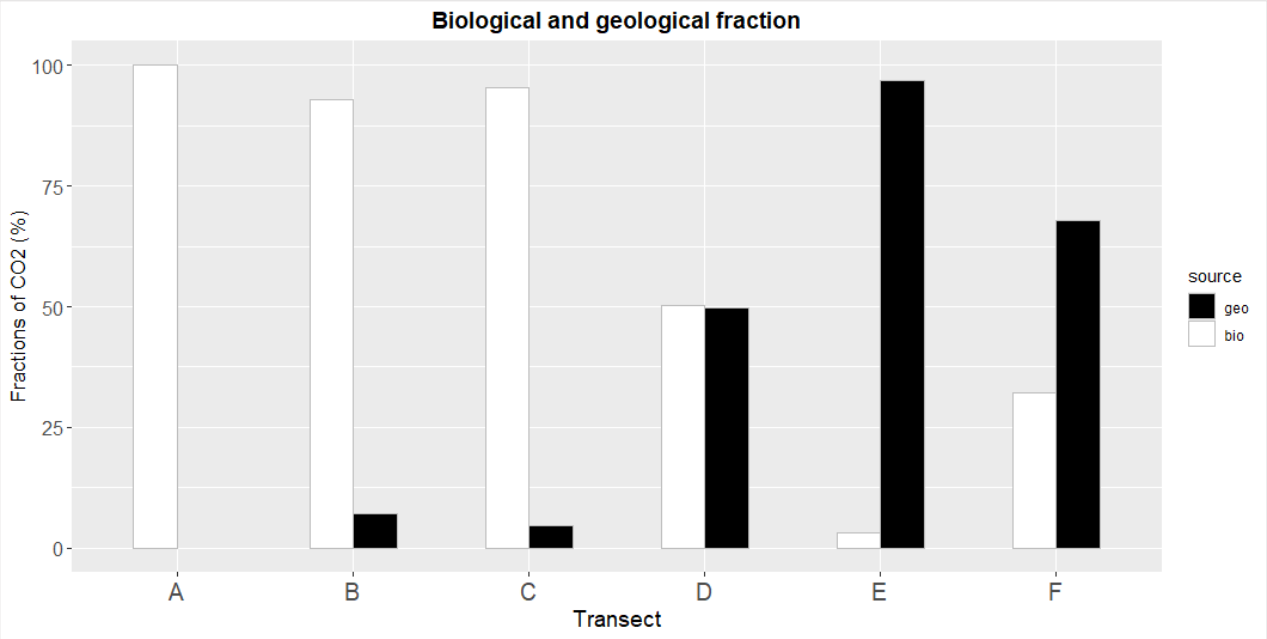

Figure 6 Fractions (in %) of biological (bio) and geological (geo) CO_2 fluxes in temperature transects A-F. The transects reflect gradually warmed soils due to geothermal activity, where A is the ambient temperature and F is the extreme warming (+30°C).

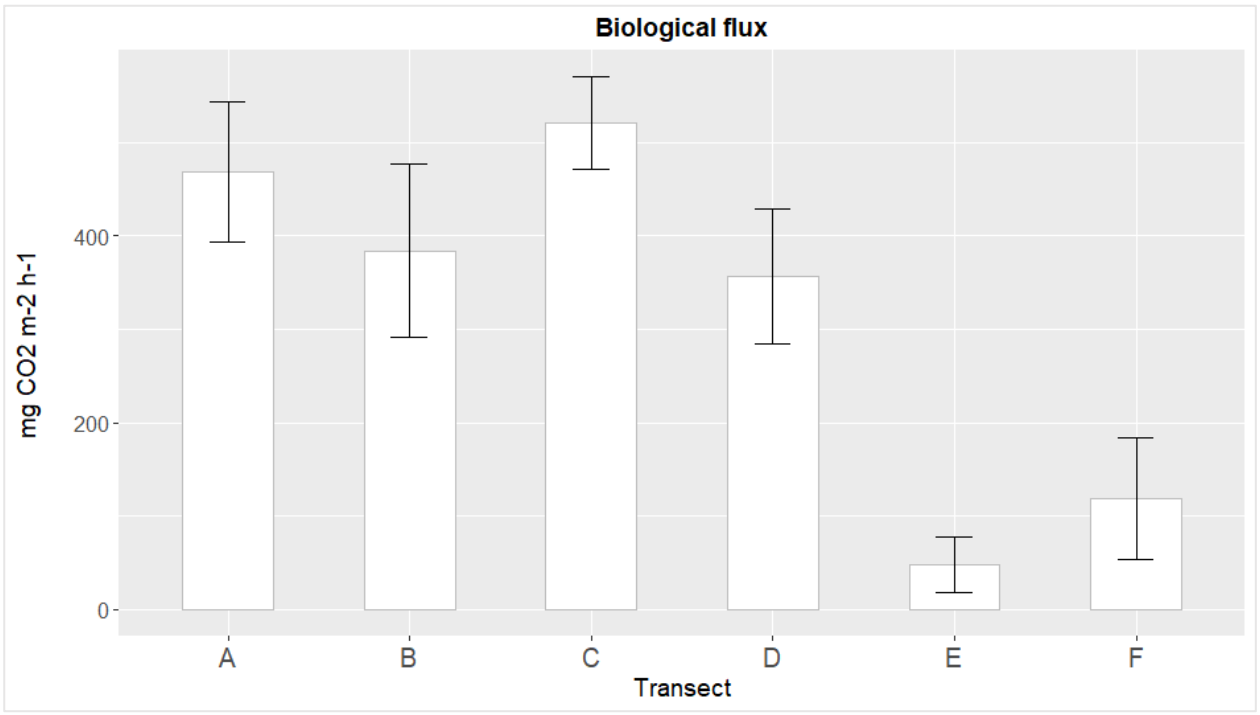

Figure 7 Biological CO_2 flux (mg CO_2 m^{-2} h^{-1}) in temperature transects A-F of a Sitka spruce forest in Iceland. The transects reflect gradually warmed soils due to geothermal activity, where A is the ambient temperature and F is the extreme warming (+30°C). Error bars represent the standard deviation.

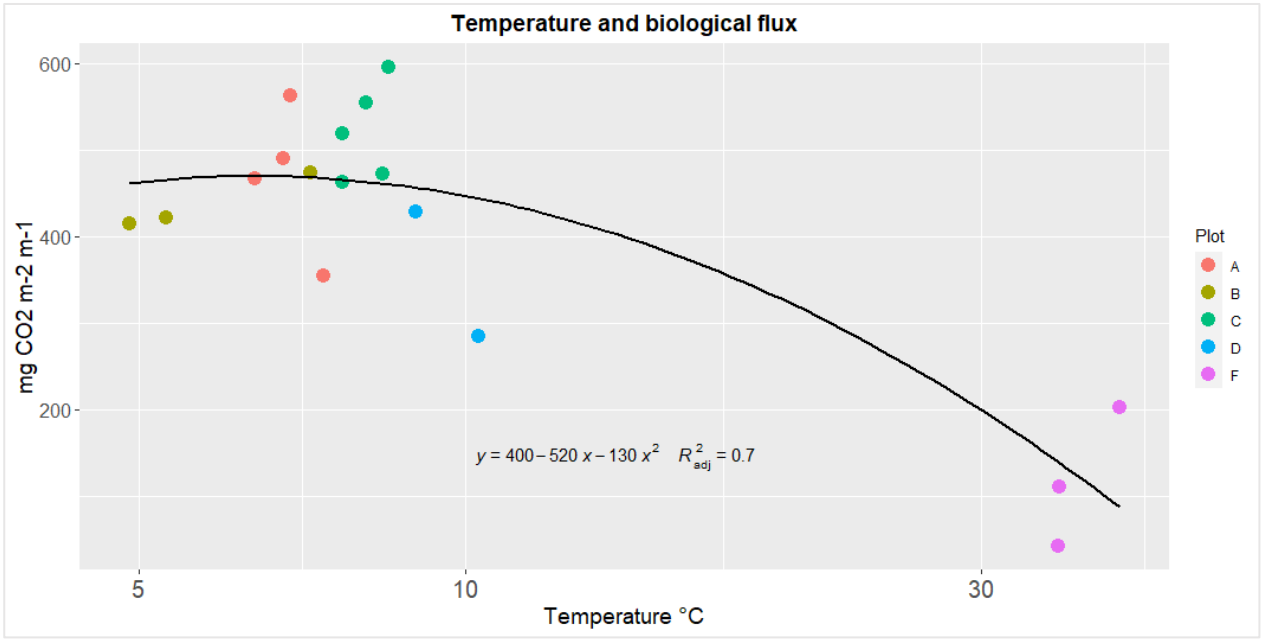

Figure 8 Temperature effects on the biological respiration rates (mg CO_2 m^{-2} h^{-1}) measured from temperature transects A-F in the geothermally warmed Sitka spruce forest of Iceland. Colours represent individual plots from each transect.

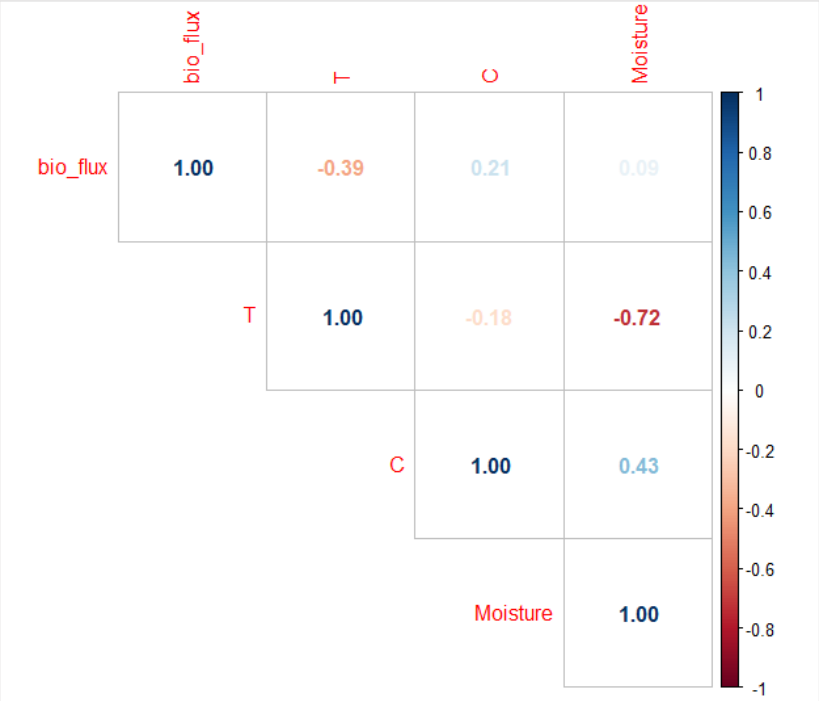

Figure 9 Correlations between biological fluxes (bio flux) measured from the geothermal temperature gradient, carbon content (C), temperature (T), and moisture. Numbers indicate the strength of Spearman correlation, further away the correlation coefficient is from zero, the stronger the correlation.

5.3.3 Soil CO_2 gas profiles and isotope results

Soil gas concentrations were measured only from transects A, D, and F. Carbon dioxide concentration in ppm along the soil profile and the increase in concentrations (slope) are presented in Figure 10. Data showed a clear increase in CO_2 concentration with increasing depth. The highest concentrations were measured from transect D at 20cm depth with 14081.80 ppm. Transect F had the lowest concentrations in 5cm depth with 2283.08 ppm. Transects D and E had a more significant increase in depth compared to transect A. There was a statistically high difference tested with Two-Way ANOVA between depths with a p-value of $2.7* 10^{-7}$ but no statistically significant difference between transect (p=0.23). There was no correlation between the concentration increase in the soil profile and the total CO_2 efflux. Concentration increase in the soil profile was similar in both D and F transects with slopes of 729 and 725, even though the total CO_2 efflux was significantly smaller in the transect F compared to D. In addition, no correlation was found between the soil CO_2 concentrations at 5cm depth and the total CO_2 flux.

The $\delta^{13}C$ values of CO_2 in the soil gas increased with the increasing temperature (figure 11), similar to the $\delta^{13}C$ values of the surface fluxes. There was hardly any variation between the depths in transect A, but for transects D and F values got more positive in the deeper layers. Values varied between -16.80‰ and -25.48‰ in transect A, between -5.73‰ and -17.90‰ for transect D, and between -1.38‰ and – 13.46‰ for transect F. The Keeling plots calculated in the soil profile are presented next to the bars for each transect measured, though some Keeling plot assumptions are violated with this approach as mentioned earlier. Accordingly, the Keeling plots of the soil CO_2 increased from -22.97‰ to -7.20‰, and to -2.29‰ from transects A to D and from D to F. In two-way ANOVA there were statistically highly significant differences in the $\delta^{13}C$ value of CO_2 between both transects ($p=2 *10^{-16}$) and depths ($p=8.3*10^{-4}$).

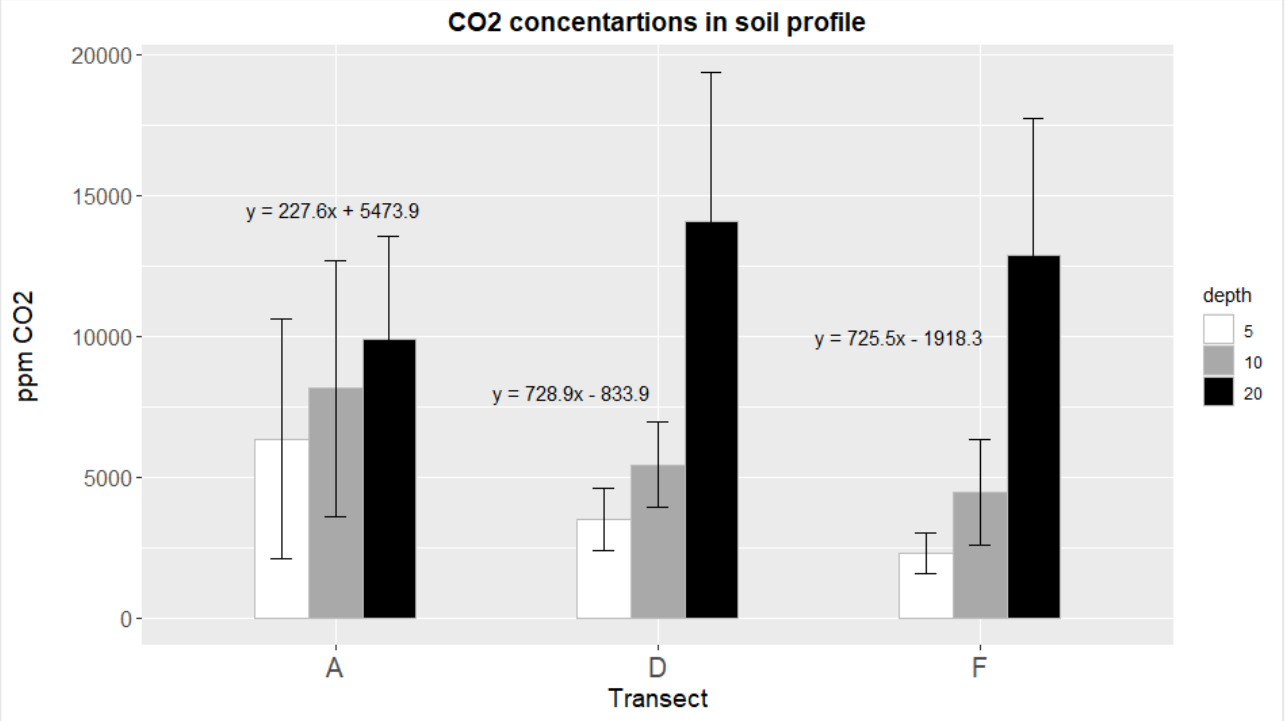

Figure 10 Soil gas profile for CO_2 from temperature transects A, D and F in the geothermally warmed Sitka spruce forest of Iceland. The transects reflect gradually warmed soils, where transect A is the ambient temperature and F is the extreme warming (+30°C). Concentrations are presented in ppm. The equation on each transect shows the increase of CO_2 concentration from 5 cm to 20 cm. Error bars represent the standard deviation.

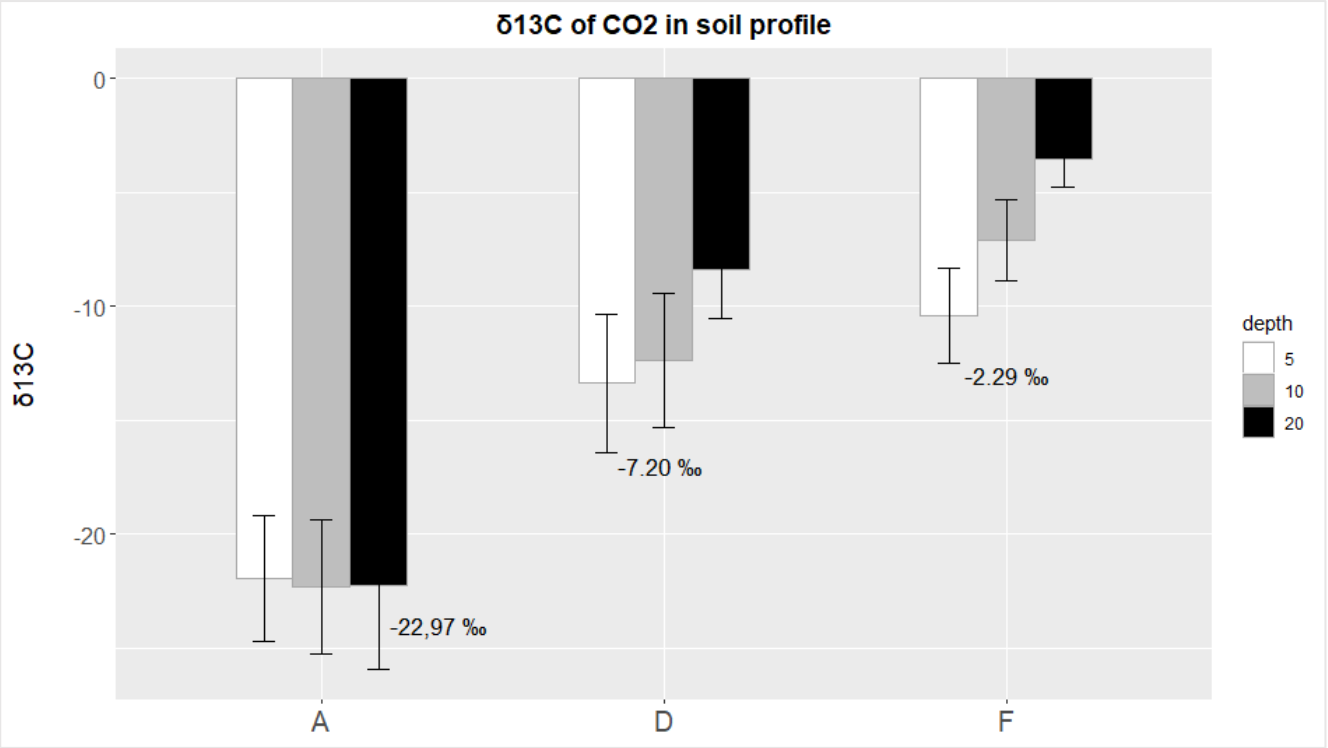

Figure 11 The δ ^{13}C values and calculated Keeling plots of CO_2 along soil profiles from temperature transects A, D and F in the geothermally warmed Sitka spruce forest of Iceland. The transects reflect gradually warmed soils, where A is the ambient temperature and F is the extreme warming (+30°C). The keeling plot calculated for each transect is shown next to the bars. Error bars represent the standard error.

5.4 Soil CH_4 fluxes and $\delta^{13}C$ values

Methane fluxes and the differences between the non-trenched and trenched plots are shown in Table 5. There were no statistically significant differences (p-value < 0.05) between the trenched and non-trenched plots for CH_4. There was a large variation in CH_4 fluxes between both trenched and non-trenched study plots. Methane fluxes in the trenched study plots ranged from -1.94 mg CH_4 m^{-2} day^{-1} (net uptake) to 2.43 mg CH_4 m^{-2} day^{-1} (emissions) (figure 12). All transects showed CH_4 uptake, except transect F. The lowest uptake rates were measured from transect C. Statistically there were significant differences in CH_4 fluxes between transects with a p-value of $2.6*10^{-4}$. In pairwise comparison (Tukey's test) only transect F had a significant difference between A ($p = 9.4*10^{-4}$), B ($p = 2.1*10^{-3}$), C ($p = 3.6*10^{-4}$), and D ($p = 8.1*10^{-4}$) transects.

Keeling plot calculations were only possible for transect F, where emissions were observed. The $\delta^{13}C$ value measured from transect F was -38.13‰ (figure 12). The mean $\delta^{13}C$ value measured from the geothermal vents (-45.25‰, see Table 1), was close to the value measured from transect F. No mixing model was applied since CH_4 can be oxidized which is against the mixing model assumption that end-member values should be spatially and temporarily invariable. Thus, the results are only qualitatively evaluated here.

Table 5 Means of CH_4 fluxes (mg $m^{-2}day^{-1}$) from trenched (n = 27) and non-trenched (n = 11) plots.

Transect	Trenched			Non-trenched			Difference
	Mean CH_4 flux (mg $m^{-2}day^{-1}$)	*SD*	*SE*	*Mean CH_4 flux (mg $m^{-2}day^{-1}$)*	*SD*	*SE*	*p-value*
A	-1.94	0.69	0.34	-1.61	-1.62	0.75	0.60
D	-1.62	1.39	0.69	-1.86	1.96	0.98	0.94
F	2.43	1.75	0.88	2.26	1.18	0.68	0.91

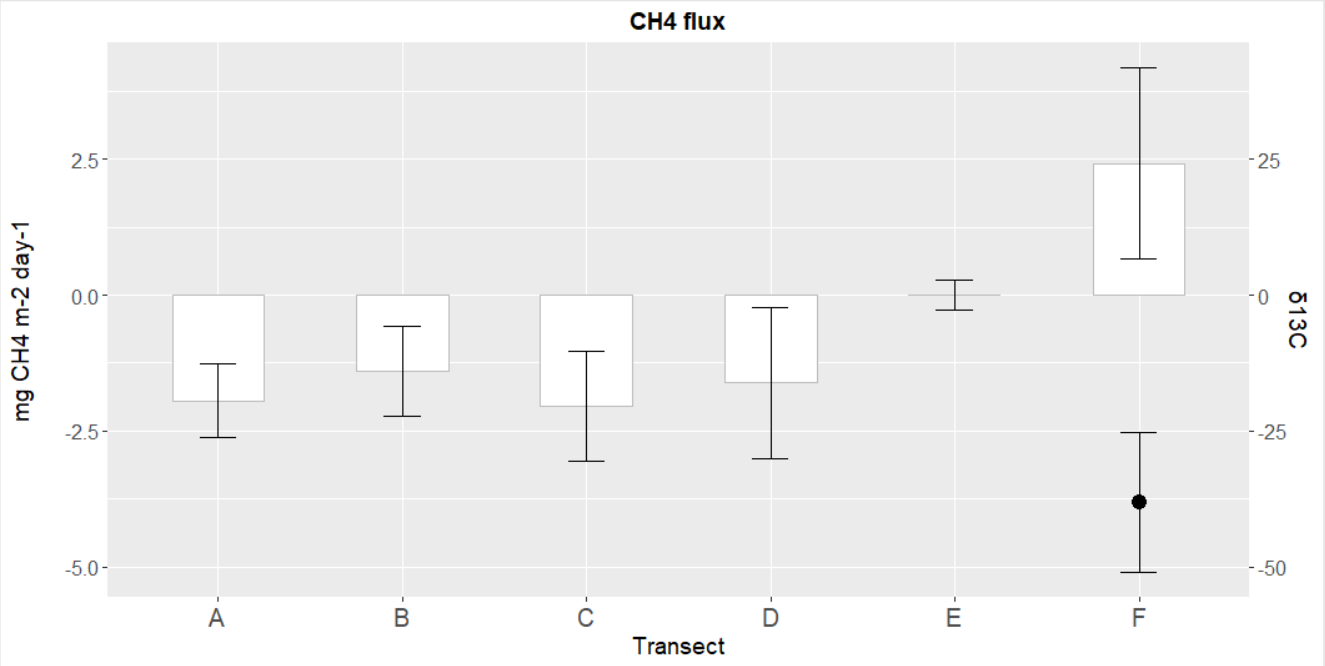

Figure 12 Mean CH_4 fluxes from temperature transects A-F in the geothermally warmed Sitka spruce forest of Iceland. The transects reflect gradually warmed soils., where A is the ambient temperature and F is the extreme warming (+30°C). Fluxes (mg $m^{-2}day^{-1}$) are presented on the left y-axis and the $\delta^{13}C$ values (‰) on the right y-axis. The $\delta^{13}C$ values could only be determined for transect F. Error bars represent the standard deviation.

5.4.1 Soil CH_4 gas profile and isotope results

Methane concentrations in soil gases are shown in Figure 13. Concentrations measured from the warmest transect (F) were significantly higher than the ones from transect A and D. Unlike CO_2 concentrations, CH_4 concentrations decreased with the increasing depth in transect A and D. In transect F, however, this pattern was reversed, and concentrations increased with the increasing depth similar to CO_2. The lowest concentrations (0.23 ppm) were measured from transect A at 20cm depth and the highest from transect F (12.4 ppm). Change in CH_4 concentrations was steeper in the D plots compared to A. There were significant differences in the CH_4 concentrations between both transects ($p = 1.02*10^{-12}$) and depths ($p = 5.6*10^{-4}$) when assessing the data with Two-Way ANOVA.

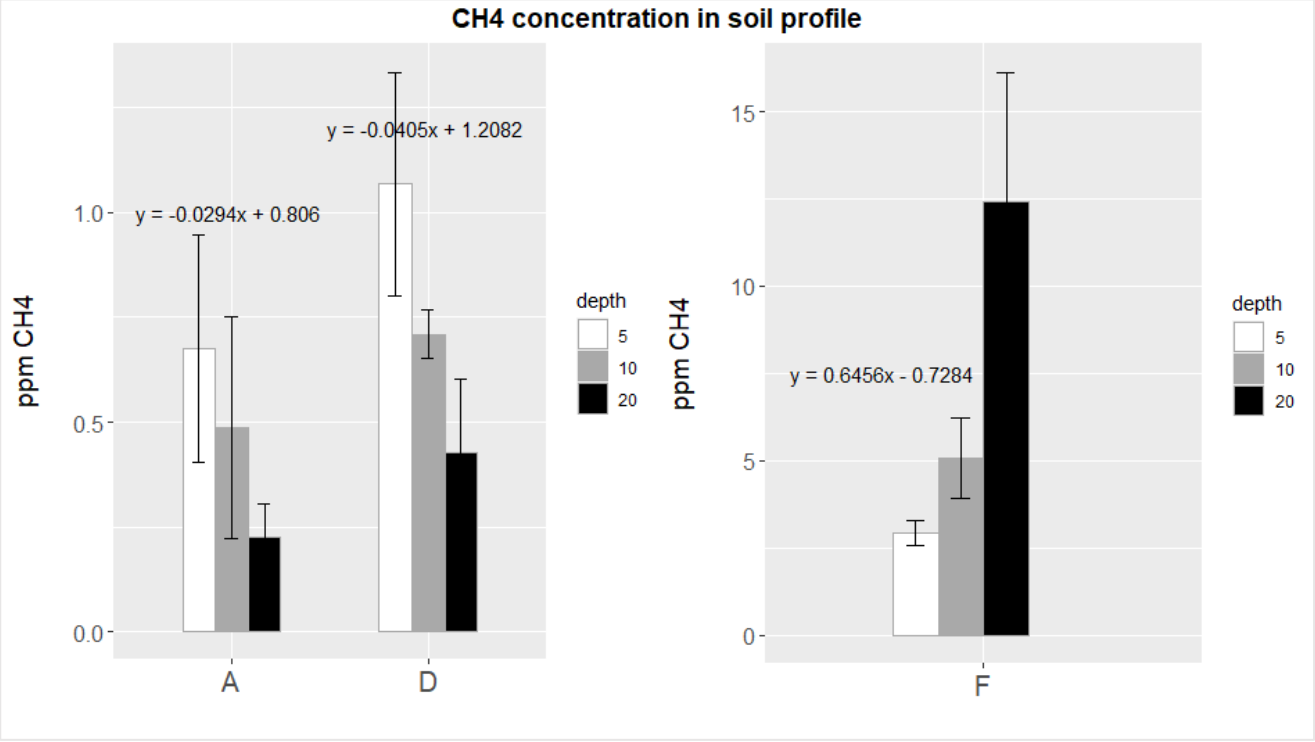

Figure 13 Soil gas profiles for CH_4 (ppm) from different temperature transects A, D and F in the Sitka spruce forest of Iceland. The transects reflect gradually warmed soils due to geothermal activity, where transect A is the ambient temperature and F is the extreme warming (+30°C). The equation on each transect shows the change of CH_4 concentration with increasing depth. Error bars represent the standard deviation.

For CH_4 the soil profile δ-values could only be interpreted from the transect F due to too low concentrations measured from the other transects (figure 14). Similarly, as for CO_2 also $\delta^{13}C$ of CH_4 got more positive in the deeper layers. The $\delta^{13}C$ values ranged from -14.49‰ to -41.90‰. The calculated Keeling plot was -12,69‰ but should be taken with caution since several assumptions are violated here. There was a statistically significant difference in the soil profile δ-values in the transect F between depths (p = 0.0387) calculated with One-Way ANOVA.

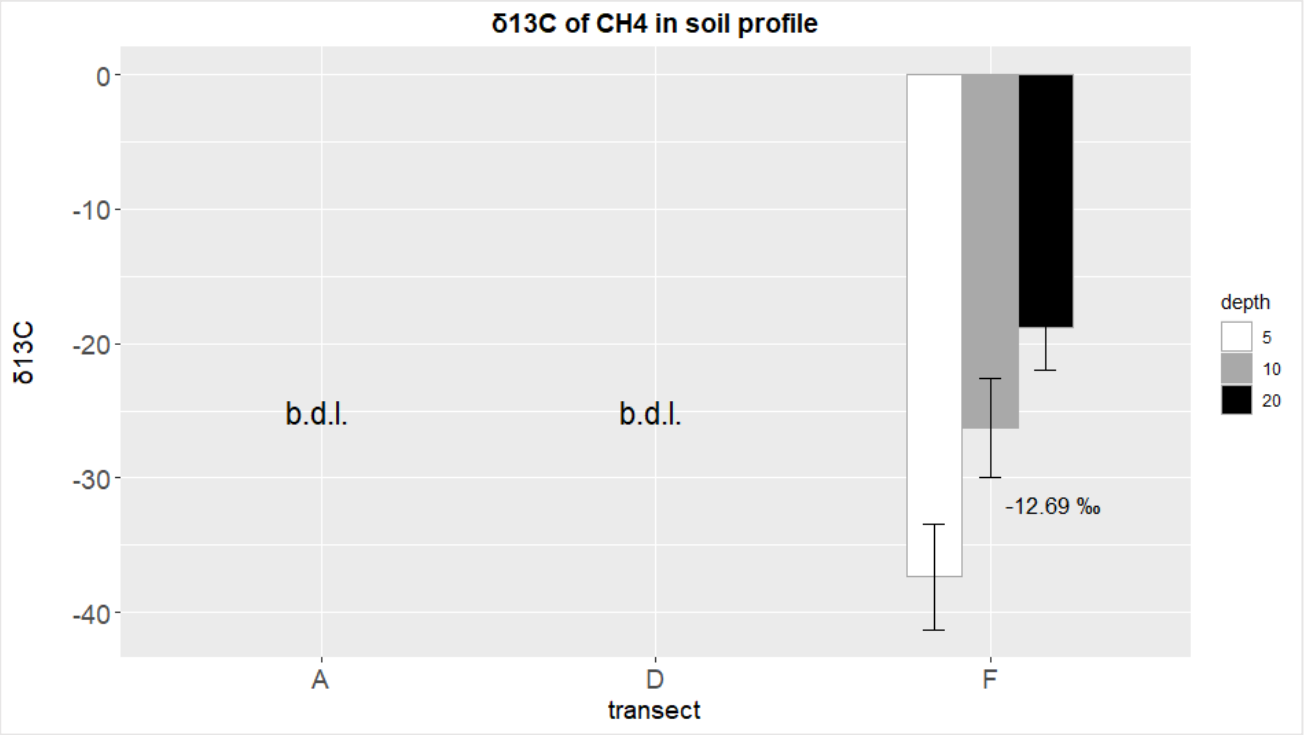

Figure 14 The $\delta^{13}C$ values of CH_4 along soil profile from temperature transects F in the geothermally warmed Sitka spruce forest of Iceland. The transects reflect gradually warmed soils, where A is the ambient temperature and F is the extreme warming (+30°C). Values are shown only for transect F since CH_4 concentrations were too low in the other transects for reliable isotope analysis. The $\delta^{13}C$ values were below the detection limit: b.d.l. for transect A and D. Calculated Keeling plot for transect F is shown next to the bars. Error bars represent the standard deviation.

6 Discussion

6.1 Soil respiration measurements in the ForHot site

In this study, the trenching method was applied to determine microbial respiration rates in a Spruce Forest in Iceland and assess its dependency on soil temperature. This is a traditional and frequently used method to measure soil respiration (Kutsch et al. 2009). Trenching was done a year before the flux measurements so that the roots had enough time to die off. Carbon dioxide fluxes measured from the trenched plots were lower in all the transects compared to the non-trenched plots (see Table 4), though differences were not always significant, indicating the reduced effect of root respiration. Also, hardly any roots were found in the trenched plots (data not shown). Thus, it can assume that the trenching method worked, and that root respiration was negligible here.

The geothermal source contributes to overall soil CO_2 emissions in the ForHOT site, and generally in volcanic areas (Maljanen et al. 2020; Tassi et al. 2015). Therefore, the source partitioning method with isotopes was applied (Maljanen et al. 2020). Carbon dioxide measured from both, surface fluxes and soil gases, was highly enriched in ^{13}C in the warmest plots, indicating a geological source (see figures 5 and 10). More positive $\delta^{13}C$ values along the warming gradients confirmed the results stated already by Maljanen et al. (2020), that there were clear geological CO_2 emissions from the geothermally warmed transects, especially in the two warmest plots E and F. This proves the importance of source identification when studying the temperature effects on microbial respiration in these geothermal temperature gradients.

In general, the relative contribution of the geothermal CO_2 flux component increased with the temperature gradient, but this increase was not linear and peaked in transect E, where the measured temperature increase was approximately + 6°C, and not the hottest transect F (+ 30 °C). Maljanen et al. (2020) measured CO_2 effluxes from the same site during two growing seasons, one in 2014 and the other in 2016. Compared to the fractions of CO_2 measured in 2016 from the same site by Maljanen et al. (2020) the fractions of biological and geological CO_2 fluxes

were similar in this study. Like in the results of this study, in the 2016 measurements, there was a noticeable, but not a tight connection between the geothermal emissions and the topsoil temperatures, unlike in 2014. Thus, geothermal CO_2 emissions get stronger with higher temperatures in these volcanic soils, but the emissions do not linearly increase with temperature. It has been shown earlier that geothermal emissions can occur also at lower temperatures and that they can occur as pulses, e.g., can be episodic (Chiodini et al. 2010).

6.2 Biological respiration

The main aim of this study was to measure biological respiration. The trenching method and isotopic mixing model was applied to meet this aim, as mentioned above. Unexpectedly, there were no statistical differences in the biological respiration rates between transects A, B, C, and D. The biological flux stayed with an average of 460 mg CO_2 m^{-2} h^{-1} at the same level between these transects. Also, the mean %C content of the soil did not change between soils of transects A - D (average of 11 %C). Transect B (+ 0.2 °C), C (+ 1.5 °C), and D (+ 2.7) are in the range of warming predicted to occur due to climate changes (IPCC 2021). The highest soil respiration was measured in transect C, but there was no significant difference to A, B or D. It seems that the effects of temperature increase on soil respiration rates are either not evident, or not measurable (e.g., differences are too small to be measured), or that fluxes are constrained by other variables.

It is considered that higher temperatures increase the microbes' energy demand, and increased energy demand leads to higher microbial respiration per soil organic carbon quantity (Marañón-Jiménez et al. 2018). It has been shown by several researchers that soil warming can accelerate microbial activity and lead to soil carbon losses (Allison et al. 2010; Bradford 2013; Frey et al. 2013; Marañón-Jiménez et al. 2018; Poeplau et al. 2020; Walker et al. 2018). This has however, been shown to occur only for a few years, after which the effects have been shown to decline (Verbrigghe et al. 2022; Walker et al. 2018; Bradford 2013; Allison et al. 2010; Frey et al. 2013). Suggested mechanisms for declining temperature effects could be related to the adaptation of microbes to higher soil temperatures (Allison et al. 2010), such as down-regulation of microbial

activity, or reduced microbial biomass (Walker et al. 2018) which operate otherwise at higher rates. Indeed, the microbial biomass in the Icelandic soils has been shown to decrease via temperature induced substrate depletion and therefore hinder the effects of increased microbial respiration rates (Allison et al. 2010; Walker et al. 2018). Walker et al. (2018) summarizes the effects as follows: "Thus, while microbial activity remains accelerated per unit of biomass; it declines per unit of soil". Verbrigghe et al. (2022) confirmed that the SOC losses occurred in the grassland site (GO and GN) only within the first five years of warming, and after that, the warming no longer reduced the SOC content. This is most likely due to the reduction of labile C stock. Poeplau et al. (2020) showed that labile C stocks were depleted during 10 years of warming when there was a slower decline in the more stable C fractions in geothermal soils. Also, the forest productivity decreases from transect A to D (Sigurðsson et al. 2019), which could result in less rhizodeposition and thus less priming of soil organic matter despite higher temperatures. Thus, there is decreased substrate supply.

The biological soil respiration significantly decreased from transects A-D to transects E and F, the warmest sites (corresponding to +5 °C and +30 °C degree warming). Generally, an increase in soil respiration rates was expected, at least in transect E. However, a significant drop in %C was observed, which could have limited soil respiration. But while %C decreased by a factor of 2 from A to E and F, soil respiration decreased by a factor of 5 to 10. Thus, the decrease in %C cannot explain the drop in respiration alone. The heterotrophic respiration rates might decrease, when exceeding the extreme temperatures, indicating that these high temperatures are beyond the optimum temperature conditions for the soil microbes adapted to the sub-arctic conditions. It has also been discussed that high geothermal CO_2 might have toxic effects on microbes (Maljanen et al. 2020), explaining the low biological respiration rates on transect E where the highest geological fluxes were measured.

In this study the soil microbial community has been exposed to soil warming for a little over 14 years, thus the system can be considered to have already shifted to a steady phase after the initial changes in the soil SOC losses in transects E and F. The minimal and statistically not significant differences in the biological respiration rates between A, B, C, and plots are more

difficult to explain, and can only be connected here to the limited substrate supply or other mechanisms such as microbial adaption, as discussed above.

6.3 Methane

There were no statistically significant differences in the CH_4 fluxes between the trenched and non-trenched plots (see Table 5), indicating that the absence of roots did not affect the total methane flux rates. Thus, the frequent CH_4 flux measurements from the trenched plots are valid. There was clear methane uptake in the transects A, B, C, and D (see figure 12), but no statistically significant differences in the mean uptake rates between these sites. Forest soils are frequently consumers of atmospheric CH_4 and show CH_4 uptake rates (Serrano-Silva et al. 2014), thus these results fit within the general literature. Methane fluxes however increased significantly in transect F, turning it into a CH_4 source. Considering only the extreme temperature (transect F) it could be stated that these results are in line with the general assumption that high temperatures and CO_2 concentration have been shown to decrease the oxidation of CH_4 and increase methanogenesis (Das and Adhya 2012). However, with these results, this cannot be stated for the lower temperature increases, since there were no differences shown between those sites (B, C, and D). Organic carbon content was significantly lower in transect F (see Table 3). Since the availability of organic matter is considered to be the controlling factor for CH_4 production (Serrano-Silva et al. 2014), it seems that emissions from transects F are mainly geological and are caused by a larger supply of geological C. Also, the isotope composition of CH_4 in transect F (-38‰) confirms this assumption, since the isotope signal was outside of any biological source (Whiticar 1999) but close to the source of the geothermal vent. Abiotic methane is generally more enriched with ^{13}C and the δ-values range between – 50‰ and -20‰ (Whiticar 1999). Thus, the assumption similar to the general scientific knowledge considering the temperature sensitivity of CH_4 fluxes, cannot be made based on the results of this study. There was no clear biological CH_4 production found. In general, CH_4 uptake has a low-temperature sensitivity compared to methane production (Serrano-Silva et al. 2014). Low-temperature sensitivity of CH_4 uptake can be considered to be the main reason why no significant changes in the uptake rates between temperatures were found.

Soil profile results from transects A and D confirm the flux results and show that CH_4 is taken up from the atmosphere in the upper layers and is not produced in the soil profile, since the concentrations decrease with the depth. For transect F the concentrations are in total significantly higher, and unlike in the other transects the concentration increases with the increasing depth, indicating the production of CH_4 at depth. The positive isotope values of CH_4 from the soil gases suggest again a geological CH_4 source. The $\delta^{13}C$ values of CH_4 are positively correlating with the increasing depth (and result in a positive Keeling plot, though general Keeling plot assumptions were violated) therefore confirming that there is more geological CH_4 present in the deeper layers.

6.4 Possible sources of error in the study and methodological consideration

There were certain shifts in the study site's temperature gradient noticed already in the previous study by Maljanen et al. (2020). There had been a minor earthquake with 2.7 on the Richter scale, on 8 July 2015. Maljanen et al. (2020) reported that the higher ends of the gradients had changed, probably due to changes in geothermal channels occurred due to this earthquake. Additionally, they observed changes between 2014 and 2016 in the higher ends of the temperature gradient. Topsoil temperatures measured in this study (see Table 2), were not directly similar to the original temperatures of each transect installed in 2014 by Sigurdsson et al. (2016), nor to the temperatures measured by Maljanen et al., causing an error when interpreting the results and indicating the variability of the geothermal system. Thus, the temperatures measured and originally assigned might not be the temperatures the soil microbes were adapted to, confounding slightly the interpretation of temperature effects on microbial activities.

The $\delta^{13}C$ values of CO_2 from volcanic sources with magmatic origin are reported to range from 0.5‰ to -2‰ (Tassi et al. 2015). In this study the source values measured from geothermal vents were around -6‰ and therefore there was possible mixing of the biological source. However, there is a huge variation for both biological and geological sources $\delta^{13}C$ values reported (Whiticar 1999). Additionally, there was no correlation between the slope of soil gas concentration

increase with depth, or the soil gas concentration and flux magnitude. This indicates that at this site, the soil gradient method cannot be considered a reliable technique when estimating the total CO_2 fluxes. It should be also noted that there was a statistically significant difference between the non-trenched and trenched plots, measured only between the plots in the transect A. Thereby it cannot be stated, that the respiration rates measured in this study from all the transects were clearly and solely heterotrophic.

In general, results from warming experiments conducted with geothermal warming cannot be extrapolated straightforwardly into the global climate scale due to limitations. Firstly, warming in the study site occurred due to the abrupt earthquake, unlike climate changes derived warming that occurs gradually. Secondly, here the soil temperature increase, not the air temperature increase, was studied. And thirdly, the study was conducted with Andosol, which is not a common soil type on a larger scale (Poeplau et al 2020). All in all, more studies considering this issue are needed to gain accurate knowledge of the climate feedback from high latitude soils.

7 Conclusions

Results of this study show that both geothermal CO_2 and CH_4 emissions get stronger with higher temperatures in volcanic soils, but the emissions do not linearly increase with temperature. The importance of source identification, when studying the temperature effects on microbial respiration in these geothermal temperature gradients was highlighted in this study. The results also confirmed that the temperature gradients originally assigned within the ForHot study site had changed during the last ten years, confounding the interpretation of temperature effects on microbial activities.

Results revealed that, unlike expected, microbial respiration rates didn't increase with increasing temperatures, and the biological fluxes stayed with an average of 460 mg CO_2 m^{-2} h^{-1} with a moderate temperature increase. It seems that the fluxes are constrained by other variables, such as reduced microbial biomass and labile C content. Additionally, high temperatures might be beyond the optimum temperature conditions for the soil microbes, or abiotic CO_2 might have toxic effects on microbes explaining the low biological respiration rates with high temperatures. However, the minimal differences in the biological respiration rates are difficult to explain.

In this study, there was no clear biological CH_4 production found and no significant differences in the CH_4 uptake rates mainly due to the low-temperature sensitivity of CH_4 uptake. More studies are required considering both CO_2 and CH_4 to be able to predict the ecological and biogeochemical responses to warming. Even though there are several limitations, the results of this thesis provide valuable insight into the adaptation of microbial respiration to a warming climate.

References

Allison, S.D., Wallenstein, M.D. & Bradford, M.A. 2010. Soil-carbon response to warming is dependent on microbial physiology. Nature Geoscience, 3, 5, pp. 336–340.

Althoff, F., Jugold, A. & Keppler, F. 2010. Methane formation by oxidation of ascorbic acid using iron minerals and hydrogen peroxide. Chemosphere, 80, 3, pp. 286–292.

Aronson, E.L. & McNulty, S.G. 2009. Appropriate experimental ecosystem warming methods by ecosystem, objective, and practicality. Agricultural and Forest Meteorology, 149, 11, pp. 1791–1799.

Ármannsson. H. 2018. An overview of carbon dioxide emissions from Icelandic geothermal areas. Applied Geochemistry, 97, pp. 11-18.

Biasi, C., Lind, S.E., Pekkarinen, N.M., Huttunen, J.T., Shurpali, N.J., Hyvönen, N.P., Repo, M.E. & Martikainen, P.J. 2008. Direct experimental evidence for the contribution of lime to CO2 release from managed peat soil. Soil Biology and Biochemistry, 40, 10, pp. 2660–2669.

Bradford, M.A. 2013. Thermal adaptation of decomposer communities in warming soils. Frontiers in Microbiology, 4, NOV.

Caddy-Retalic, S., Andersen, A.N., Aspinwall, M.J., Breed, M.F., Byrne, M., Christmas, M.J., Dong, N., Evans, B.J., Fordham, D.A., Guerin, G.R., Hoffmann, A.A., Hughes, A.C., van Leeuwen, S.J., McInerney, F.A., Prober, S.M., Rossetto, M., Rymer, P.D., Steane, D.A., Wardle, G.M. & Lowe, A.J. 2017. Bioclimatic transect networks: Powerful observatories of ecological change. Ecology and Evolution, 7, 13, pp. 4607–4619.

Chiodini, G., Granieri, D., Avino, R., Caliro, S., Costa, A., Minopoli, C. & Vilardo, G. 2010. Non-volcanic CO2 Earth degassing: Case of Mefite d'Ansanto (southern Apennines), Italy. Geophysical Research Letters, 37, 11.

Das, S. & Adhya, T.K. 2012. Dynamics of methanogenesis and methanotrophy in tropical paddy soils as influenced by elevated CO 2 and temperature interaction. Soil Biology and Biochemistry, 47, pp. 36–45.

Dawson, T.E. & Siegwolf, R. 2007. Stable Isotopes As Indicators of Ecological Change. Elsevier Science & Technology. Amsterdam.

Eckhardt, Tim; Kutzbach, Lars (2016): MATLAB code to calculate gas fluxes from chamber-based methods. Institut für Bodenkunde, Universität Hamburg, PANGAEA.

Etiope, G. & Sherwood Lollar, B. 2013. Abiotic methane on earth. Reviews of Geophysics, 51, 2, pp. 276–299.

ForHot. 2021. ForHot, Agricultural University of Iceland. https://forhot.is/. Accessed 3.4.2022.

von Fischer, J.C. & Hedin, L.O. 2007. Controls on soil methane fluxes: Tests of biophysical mechanisms using table isotope tracers. Global Biogeochemical Cycles, 21, 2.

Fischer, T.P., Arellano, S., Carn, S., Aiuppa, A., Galle, B., Allard, P., Lopez, T., Shinohara, H., Kelly, P., Werner, C., Cardellini, C. & Chiodini, G. 2019. The emissions of CO2 and other volatiles from the world's subaerial volcanoes. Scientific Reports, 9, 1.

de Frenne, P., Graae, B.J., Rodríguez-Sánchez, F., Kolb, A., Chabrerie, O., Decocq, G., de Kort, H., de Schrijver, A., Diekmann, M., Eriksson, O., Gruwez, R., Hermy, M., Lenoir, J., Plue, J., Coomes, D.A. & Verheyen, K. 2013. Latitudinal gradients as natural laboratories to infer species' responses to temperature. Journal of Ecology, 101, 3, pp. 784–795.

Frey, S.D., Lee, J., Melillo, J.M. & Six, J. 2013. The temperature response of soil microbial efficiency and its feedback to climate. Nature Climate Change, 3, 4, pp. 395–398.

Helsingin yliopisto. 2013. Eddy Covariance. https://www.atm.helsinki.fi/Eddy_Covariance/. Accessed 11.7.2022.

Hollister, R.D., Elphinstone, C., Henry, G.H., Bjorkman, A.D., Klanderud, K., Björk, R.G., Björkman, M.P., Bokhorst, S., Carbognani, M., Cooper, E.J. and Dorrepaal, E. 2022. A review of open top chamber (OTC) performance across the ITEX Network. Arctic Science.

Hugelius, G., Strauss, J., Zubrzycki, S., Harden, J.W., Schuur, E.A.G., Ping, C.L., Schirrmeister, L., Grosse, G., Michaelson, G.J., Koven, C.D., O'Donnell, J.A., Elberling, B., Mishra, U., Camill, P., Yu, Z., Palmtag, J. & Kuhry, P. 2014. Estimated stocks of circumpolar permafrost carbon with quantified uncertainty ranges and identified data gaps. Biogeosciences, 11, 23, pp. 6573–6593.

Hutchinson, G.L., Livingston, G.P., Healy, R.W. and Striegl, R.G. 2000. Chamber measurement of surface-atmosphere trace gas exchange: Numerical evaluation of dependence on soil, interfacial layer, and source/sink properties. Journal of Geophysical Research: Atmospheres, 105(D7), pp.8865-8875.

IPCC. 2021. Summary for Policymakers. In: Climate Change 2021: The Physical Science Basis. Contribution of Working Group I to the Sixth Assessment Report of the Intergovernmental Panel on Climate Change [Masson-Delmotte, V., P. Zhai, A. Pirani, S.L. Connors, C. Péan, S. Berger, N. Caud, Y. Chen, L. Goldfarb, M.I. Gomis, M. Huang, K. Leitzell, E. Lonnoy, J.B.R. Matthews, T.K. Maycock, T. Waterfield, O. Yelekçi, R. Yu, and B. Zhou (eds.)]. Cambridge University Press, Cambridge, United Kingdom and New York, NY, USA, pp. 3−32.

IPCC. 2022. Summary for Policymakers. In: Climate Change 2022: Impacts, Adaptation, and Vulnerability. Contribution of Working Group II to the Sixth Assessment Report of the Intergovernmental Panel on Climate Change [H.-O. Pörtner, D.C. Roberts, M. Tignor, E.S.

Poloczanska, K. Mintenbeck, A. Alegría, M. Craig, S. Langsdorf, S. Löschke, V. Möller, A. Okem, B. Rama (eds.)]. Cambridge University Press, Cambridge, UK and New York, NY, USA, pp. 3-33.

Kammann, C., Hepp, S., Lenhart, K. & Müller, C. 2009. Stimulation of methane consumption by endogenous CH4 production in aerobic grassland soil. Soil Biology and Biochemistry, 41, 3, pp. 622–629.

Keeling, C.D. 1958. The concentration and isotopic abundances of atmospheric carbon dioxide in rural areas.

Kondo, M., Patra, P.K., Sitch, S., Friedlingstein, P., Poulter, B., Chevallier, F., Ciais, P., Canadell, J.G., Bastos, A., Lauerwald, R., Calle, L., Ichii, K., Anthoni, P., Arneth, A., Haverd, V., Jain, A.K., Kato, E., Kautz, M., Law, R.M., Lienert, S., Lombardozzi, D., Maki, T., Nakamura, T., Peylin, P., Rödenbeck, C., Zhuravlev, R., Saeki, T., Tian, H., Zhu, D. & Ziehn, T. 2020. State of the science in reconciling top-down and bottom-up approaches for terrestrial CO2 budget. Global Change Biology, 26, 3, pp. 1068–1084.

Kutsch, W.L., Bahn, M. & Heinemeyer, A. 2009. Soil carbon dynamics : an integrated methodology. Cambridge University Press. Cambridge, UK.

Kuzyakov, Y. 2006. Sources of CO2 efflux from soil and review of partitioning methods. Soil biology & biochemistry, 38, 3, pp. 425–448.

Lal, R. 2007. Carbon Management in Agricultural Soils. Mitigation and Adaptation Strategies for Global Change,12, pp. 303–322.

Lei, J., Guo, X., Zeng, Y., Zhou, J., Gao, Q. & Yang, Y. 2021. Temporal changes in global soil respiration since 1987. Nature Communications, 12, 1.

Li-Cor. 2022. Trace Gas Analyzers. https://www.licor.com/env/products/trace_gas/index. Accessed 6.11.2022.

Luo, Yiqi. & Zhou, Xuhui. 2006. Soil respiration and the environment. Elsevier Academic Press. Amsterdam.

Maier, M. & Schack-Kirchner, H. 2014. Using the gradient method to determine soil gas flux: A review. Agricultural and Forest Meteorology, 192–193, pp. 78–95.

Majlesi, S., Juutilainen, J., Trubnikova, T. & Biasi, C. 2020. Content of soil-derived carbon in soil biota and fauna living near soil surface: Implications for radioactive waste. Journal of Environmental Radioactivity, 225.

Maljanen, M., Bhattarai, H. R., Biasi, C. & Sigurdsson, B.D. 2018. The effect of geothermal soil warming on the production of carbon dioxide (CO 2), methane (CH 4), nitrous oxide (N 2 O),

nitric oxide (NO) and nitrous acid (HONO) from forest soil in southern Iceland. Icelandic Agricultural Sciences, 31,1, pp.11–22.

Maljanen, M., Yli-Moijala, H., Sigurdsson, B.D. & Biasi, C. 2020. Stable isotope method reveals the role of abiotic source of carbon dioxide efflux from geothermally warmed soil in southern Iceland. Icelandic Agricultural Sciences, 33, pp. 41–56.

Marañón-Jiménez, S., Soong, J.L., Leblans, N.I.W., Sigurdsson, B.D., Peñuelas, J., Richter, A., Asensio, D., Fransen, E. & Janssens, I.A. 2018. Geothermally warmed soils reveal persistent increases in the respiratory costs of soil microbes contributing to substantial C losses. Biogeochemistry, 138, 3, pp. 245–260.

Marushchak, M.E., Kerttula, J., Diáková, K., Faguet, A., Gil, J., Grosse, G., Knoblauch, C., Lashchinskiy, N., Martikainen, P.J., Morgenstern, A. & Nykamb, M. 2021. Thawing Yedoma permafrost is a neglected nitrous oxide source. Nature communications, 12,1, pp.1-10.

Monteith, J. & Unsworth, M. 2013. Principles of Environmental Physics: Plants, Animals, and the Atmosphere. Elsevier Science & Technology. Jordan Hill.

Nahlik, A.M. & Fennessy, M.S. 2016. Carbon storage in US wetlands. Nature Communications, 7.

O'Gorman, E.J., Benstead, J.P., Cross, W.F., Friberg, N., Hood, J.M., Johnson, P.W., Sigurdsson, B.D. & Woodward, G. 2014. Climate change and geothermal ecosystems: Natural laboratories, sentinel systems, and future refugia. Global Change Biology, 20, 11, pp. 3291–3299.

Peterson, B.J. & Fry, B. 1987. Stable Isotopes in Ecosystem Studies.

Poeplau, C., Sigurdsson, P. & Sigurdsson, B.D. 2020. Depletion of soil carbon and aggregation after strong warming of a subarctic Andosol under forest and grassland cover. SOIL, 6, 1, pp. 115–129.

Rantanen, M., Karpechko, A.Y., Lipponen, A., Nordling, K., Hyvärinen, O., Ruosteenoja, K., Vihma, T. & Laaksonen, A., 2022. The Arctic has warmed nearly four times faster than the globe since 1979. Communications Earth & Environment, 3,1, pp.1-10.

Reay, D., Smith, P. & Amstel, A. van. 2010. Methane and climate change. London: Earthscan.

Riebeek, H. 2011. The Carbon Cycle. Earth observatory. https://earthobservatory.nasa.gov/features/CarbonCycle. Accessed 12.6.2022.

Romero-Olivares, A.L., Allison, S.D. & Treseder, K.K. 2017. Soil microbes and their response to experimental warming over time: A meta-analysis of field studies. Soil Biology and Biochemistry, 107, pp. 32–40.

Scott, M. & Lindsey R. 2016. Which emits more carbon dioxide: volcanoes or human activities. https://www.climate.gov/news-features/climate-qa/which-emits-more-carbon-dioxide-volcanoes-or-human-activities. Accessed 8.8.2022.

Serrano-Silva, N., Sarria-Guzm´an, Y., Guzm´an, G., Dendooven, L. & Luna-Guido, M. 2014. Methanogenesis and Methanotrophy in Soil: A Review * 1.

Sigurdsson, B.D., Leblans, N.I.W., Dauwe, S., Gudmundsdóttir, E., Gundersen, P., Gunnarsdóttir, G.E., Holmstrup, M., Ilieva-Makulec, K., Kätterer, T., Marteinsdóttir, B., Maljanen, M., Oddsdóttir, E.S., Ostonen, I., Peñuelas, J., Poeplau, C., Richter, A., Sigurdsson, P., van Bodegom, P., Wallander, H., Weedon, J. & Janssens, I. 2016. Geothermal ecosystems as natural climate change experiments: The ForHot research site in Iceland as a case study. Icelandic Agricultural Sciences, 29, 1, pp. 53–71.

Sigurðsson, P., Oddsdóttir, E.S., Ostonen, I. & Sigurðsson, B.D. 2019. FORHOT-FOREST Final Report-1.2 Research Overview.

Subke, J.A., Kutzbach, L. & Risk, D., 2021. Soil Chamber Measurements. In Springer Handbook of Atmospheric Measurements, Springer, pp. 1607-1624.

Tassi, F., Venturi, S., Cabassi, J., Vaselli, O., Gelli, I., Cinti, D. & Capecchiacci, F. 2015. Biodegradation of CO2, CH4 and volatile organic compounds (VOCs) in soil gas from the Vicano–Cimino hydrothermal system (central Italy). Organic Geochemistry, 86, pp. 81–93.

Verbrigghe, N., Leblans, N.I.W., Sigurdsson, B.D., Vicca, S., Fang, C., Fuchslueger, L., Soong, J.L., Weedon, J.T., Poeplau, C., Ariza-Carricondo, C., Bahn, M., Guenet, B., Gundersen, P., Gunnarsdóttir, G.E., Kätterer, T., Liu, Z., Maljanen, M., Marañón-Jiménez, S., Meeran, K., Oddsdóttir, E.S., Ostonen, I., Peñuelas, J., Richter, A., Sardans, J., Sigurðsson, P., Torn, M.S., van Bodegom, P.M., Verbruggen, E., Walker, T.W.N., Wallander, H. & Janssens, I.A. 2022. Soil carbon loss in warmed subarctic grasslands is rapid and restricted to topsoil. Biogeosciences, 19, 14, pp. 3381–3393.

Virkkala, A.M., Aalto, J., Rogers, B.M., Tagesson, T., Treat, C.C., Natali, S.M., Watts, J.D., Potter, S., Lehtonen, A., Mauritz, M. and Schuur, E.A., 2021. Statistical upscaling of ecosystem CO2 fluxes across the terrestrial tundra and boreal domain: Regional patterns and uncertainties. Global Change Biology, 27,17, pp.4040-4059.

Walker, T.W.N., Kaiser, C., Strasser, F., Herbold, C.W., Leblans, N.I.W., Woebken, D., Janssens, I.A., Sigurdsson, B.D. & Richter, A. 2018. Microbial temperature sensitivity and biomass change explain soil carbon loss with warming. Nature Climate Change, 8, 10, pp. 885–889.

Wei, T. & Simko, V. 2021. R package 'corrplot': Visualization of a Correlation Matrix. (Version 0.92), https://github.com/taiyun/corrplot.

Whiticar, M.J. 1999. Carbon and hydrogen isotope systematics of bacterial formation and oxidation of methane. Chemical Geology, 161, 1-3, pp. 291–314.

Appendix

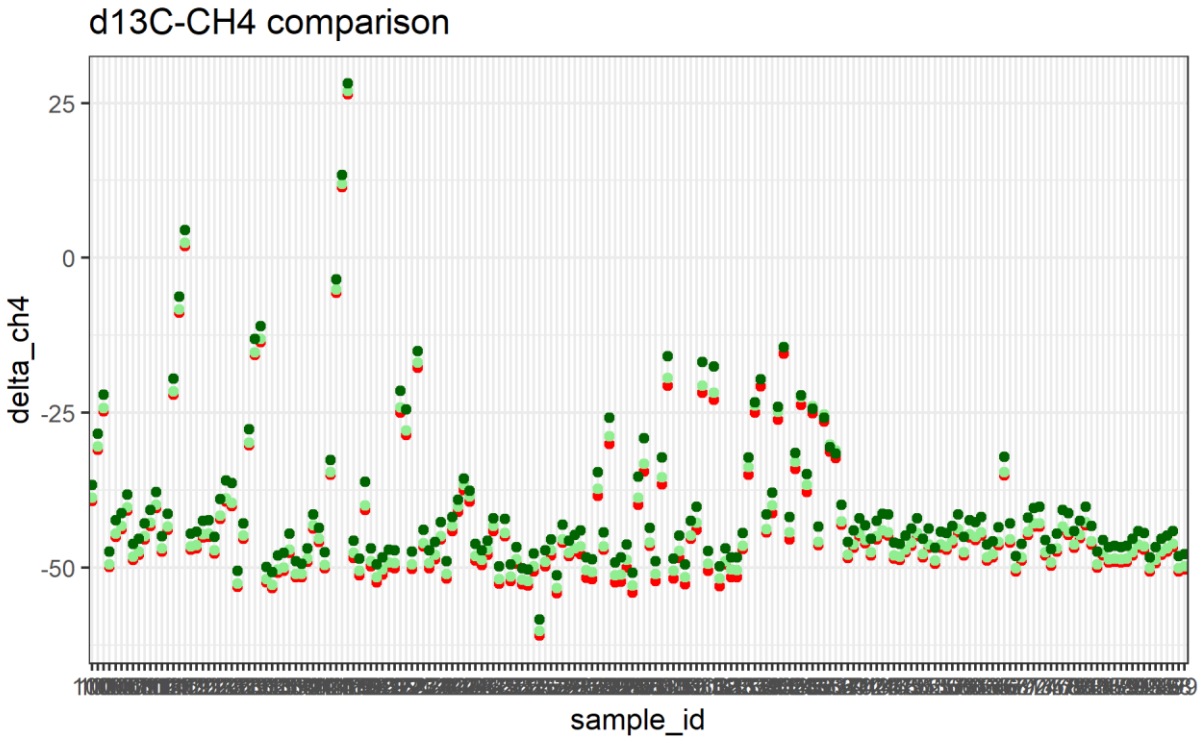
d13C-CH4 comparison
25
0
-25
-50
delta_ch4
sample_id

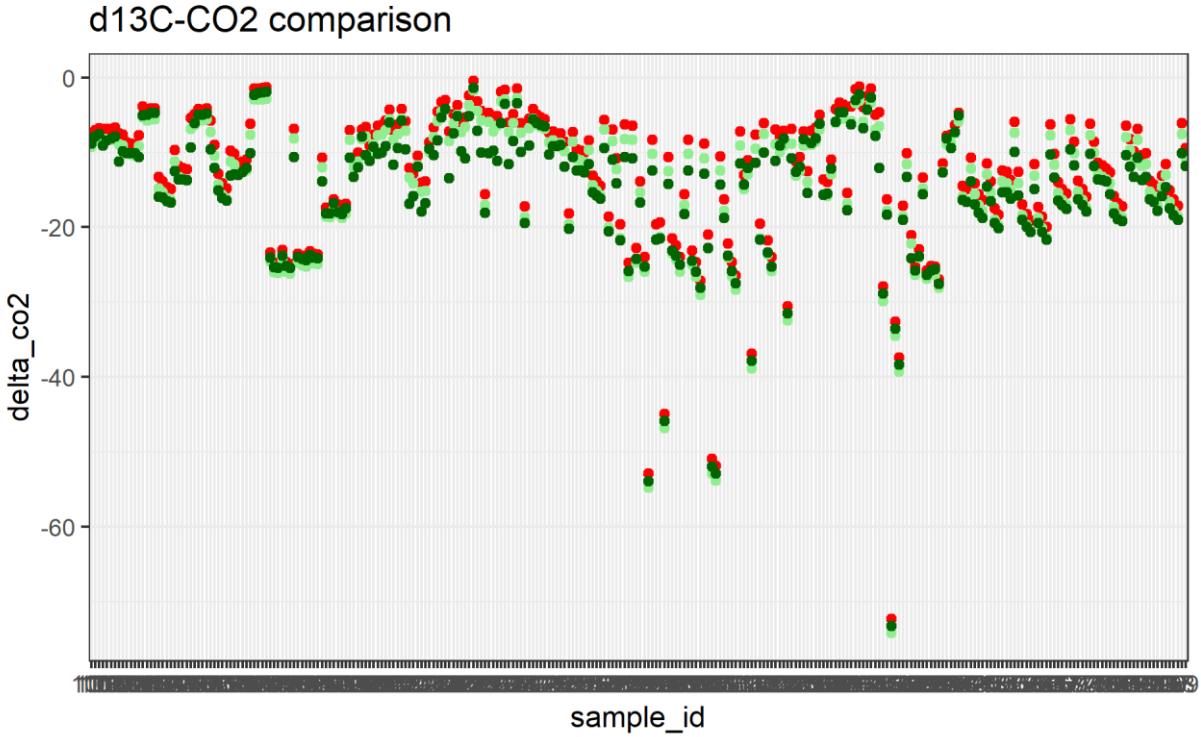
d13C-CO2 comparison
0
-20
-40
-60
delta_co2
sample_id

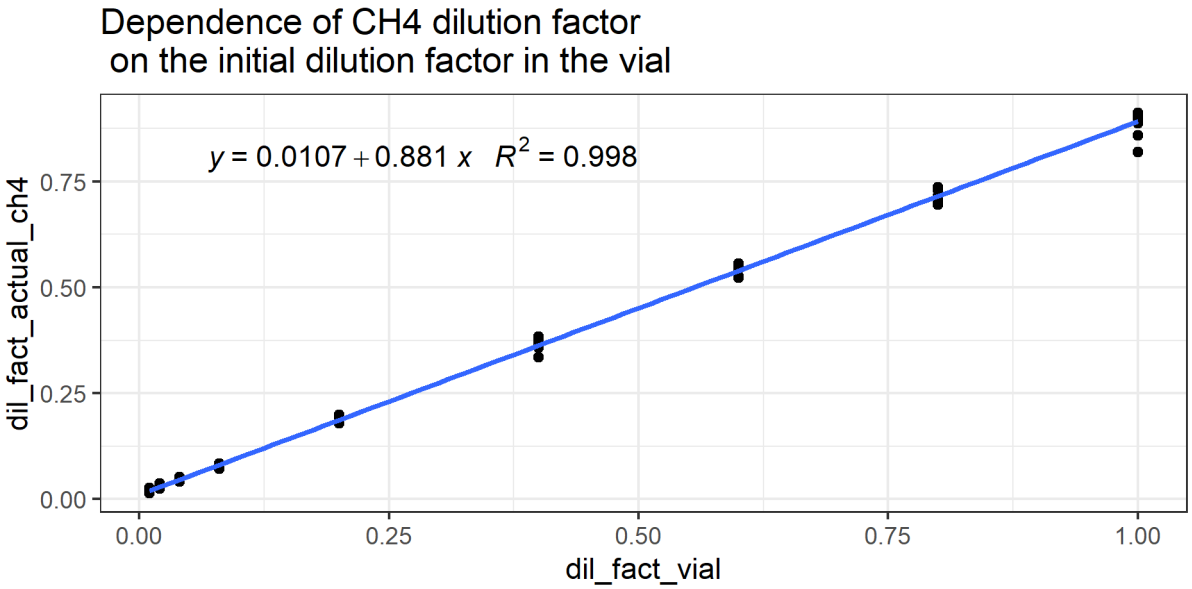
Dependence of CH4 dilution factor
on the initial dilution factor in the vial
y = 0.0107 + 0.881 x R2 = 0.998
dil_fact_actual_ch4
0.00
0.25
0.50
0.75
dil_fact_vial
0.00
0.25
0.50
0.75
1.00

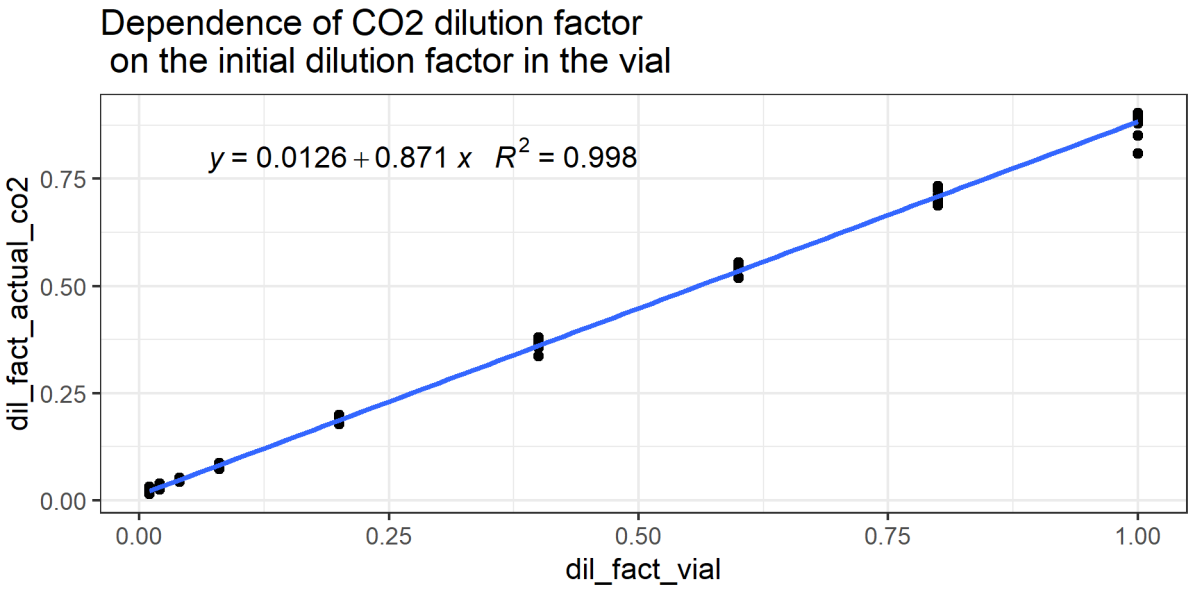
Dependence of CO2 dilution factor
on the initial dilution factor in the vial
y = 0.0126 + 0.871 x R2 = 0.998
dil_fact_actual_co2
0.00
0.25
0.50
0.75
dil_fact_vial
0.00
0.25
0.50
0.75
1.00

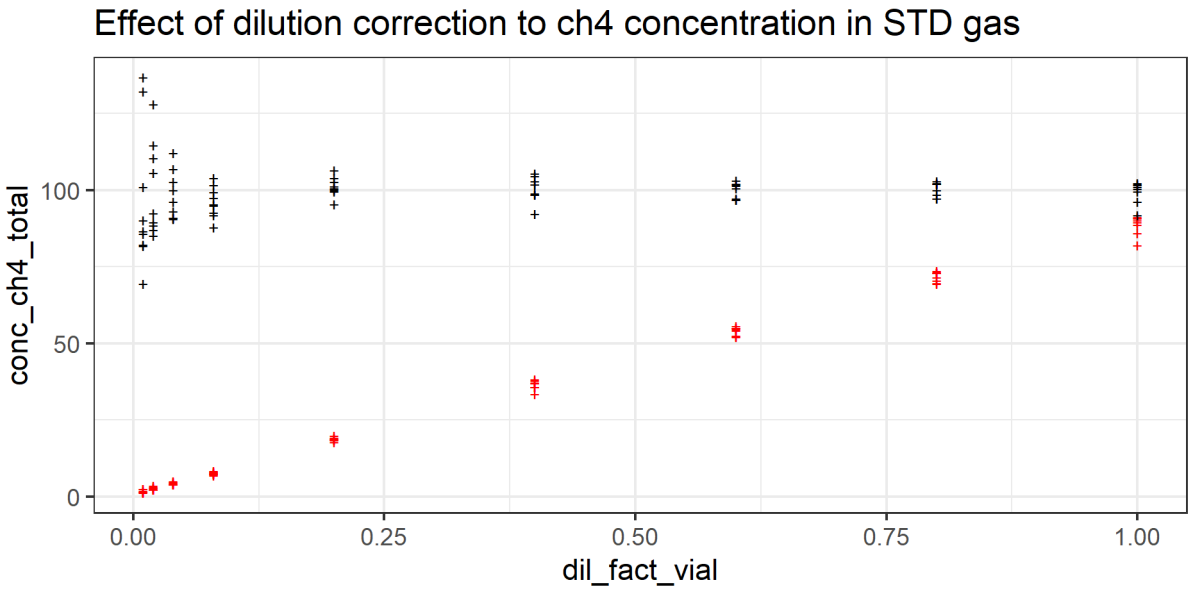
Effect of dilution correction to ch4 concentration in STD gas
conc_ch4_total
100
50
0
0.00
0.25
0.50
0.75
1.00
dil_fact_vial

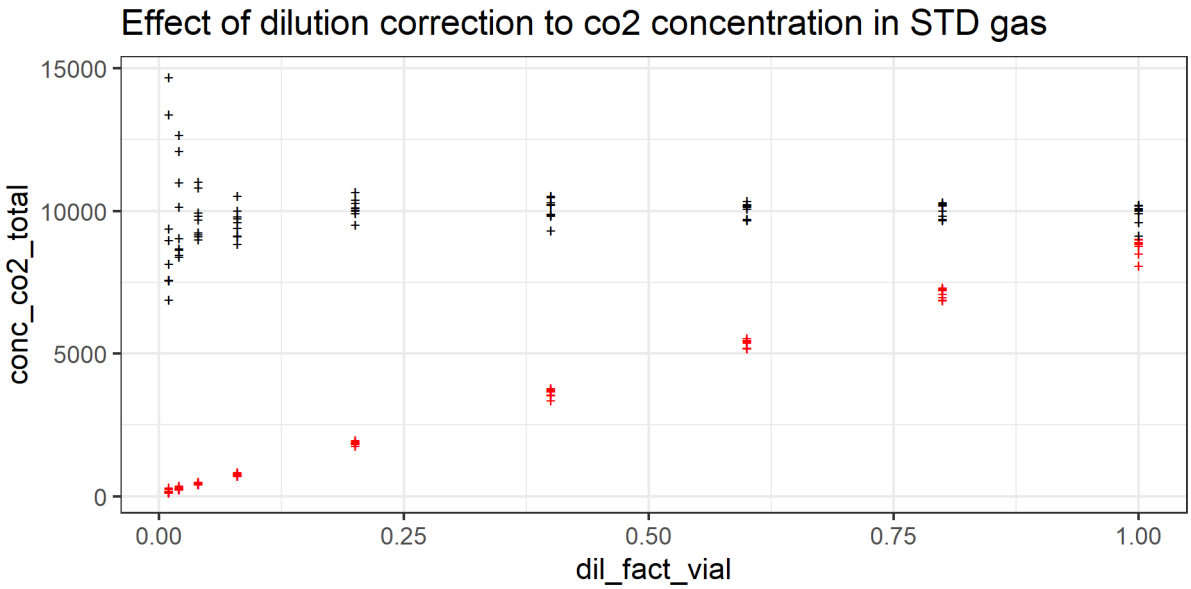
Effect of dilution correction to co2 concentration in STD gas
conc_co2_total
15000
10000
5000
0
0.00
0.25
0.50
0.75
1.00
dil_fact_vial